

ИНСТИТУТ ЗА ФИЗИКУ

ПРИМЛ ЕНО:		12. 04. 2019	
Рад.јед.	б р о ј	Арх.шифра	Прилог
0401	534/7		

Научно веће

Институт за физику у Београду

ПРЕДМЕТ: Молба за покретање поступка за реизбор у звање истраживач сарадник

Молим Научно веће Института за физику да у складу са Правилником о поступку и начину вредновања и квантитативном исказивању научно-истраживачких резултата покрене поступак за мој реизбор у звање истраживач сарадник. У прилогу достављам:

1. Мишљење руководиоца
2. Стручну биографију
3. Преглед научне активности
4. Списак и копије објављених научних радова
5. Уверење о последњем уписаном и овереном семестру
6. Уверење о завршеним основним академским студијама
7. Потврду о прихватању предлога теме докторске дисертације.
8. Додатак

У Београду, 12.04.2019. године

С поштовањем,

Јасмина Лазаревић

Јасмина Лазаревић, истраживач сарадник

ИНСТИТУТ ЗА ФИЗИКУ			
ПРИМЛ ЕНО:		12. 04. 2019	
Рад.јед.	б р о ј	Арх.шифра	Прилог
0801	534/2		

НАУЧНО ВЕЋЕ

ИНСТИТУТ ЗА ФИЗИКУ

ПРЕДМЕТ: Мишљење руководиоца Центра за физику чврстог стања и нове материјале

Јасмина Лазаревић, дипломирани фармацеут, запослена је у Центру за физику чврстог стања и нове материјале Института за физику од 1.5.2018. године. Ангажована је на пројекту Министарства просвете, науке и технолошког развоја број ИИИ46010 од 1.12.2013. Студент је пете године докторских студија на Технолошко-металуршком факултету Универзитета у Београду на смеру Биохемијско инжењерство и биотехнологија. У звање истраживач сарадник изабрана је 4.6.2015. године. Током 2016. и 2017. године колегиница Јасмина Лазаревић провела је 12 месеци на породилском боловању и боловању ради неге детета.

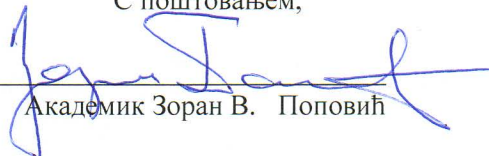
Област научно-истраживачког рада Јасмине Лазаревић је примена Раманове спектроскопије у анализи фармаколошки активних супстанци и биолошких/биотехнолошких узорака. До сада, кандидаткиња је објавила две публикације у врхунском међународном часопису (M21), једну у истакнутом међународном часопису (M22), као и саопштење на међународној конференцији штампано у изводу (M34). Веће научних области техничких наука, Универзитета у Београду дало је сагласност на предлог теме докторске дисертације Јасмине Лазаревић, под називом: „Раманова спектроскопија фармаколошки активних супстанци и биокатализатора“.

Будући да кандидаткиња задовољава услове прописане Правилником о поступку и начину вредновања и квантитативном исказивању научно-истраживачких резултата Министарства просвете, науке и технолошког развоја, предлажем реизбор Јасмине Лазаревић у звање истраживач сарадник. За чланове комисије за реизбор Јасмине Лазаревић у звање истраживач сарадник предлажем:

1. Др Урош Ралевић, научни сарадник, Институт за физику у Београду
2. Др Милош Радоњић, научни сарадник, Институт за физику у Београду
3. Проф. др Бранко Бугарски, редовни професор, Универзитет у Београду, Технолошко-металуршки факултет
4. Академик Зоран В. Поповић, научни саветник, Институт за физику у Београду.

У Београду, 12.04.2019. године.

С поштовањем,


Академик Зоран В. Поповић

Стручна биографија

Јасмина Ј. Лазаревић је рођена 05.10.1985. године у Београду. Основну школу и гимназију завршила је у Зрењанину. Школске 2004/2005. године уписала је основне академске студије на Фармацеутском факултету Универзитета у Београду, смер дипломирани фармацеут. Дипломирала је у априлу 2011. године са радом под називом „Примена раманске спектроскопије у фармацији“. Након обавезног једногодишњег приправничког стажа (Апотека Београд-Свети Сава, апотека специјалне болнице за плућне болести Др Васа Савић, Зрењанин) и положеног стручног испита за фармацеуте, школске 2012/2013. године запослена је као сарадник у настави на Катедри за аналитичку хемију Фармацеутског факултета Универзитета у Београду, где је ангажована на припреми и извођењу практичне наставе и пратећих активности на неколико обавезних и изборних предмета. Докторске академске студије уписала је на Технолошко-металуршком факултету Универзитета у Београду школске 2013/2014. године, студијски програм Биохемијско инжењерство и биотехнологија, које и даље похађа. Положила је све испите предвиђене планом и програмом. Научно-истраживачку активност започела је децембра 2013. године у Иновационом центру Технолошко-металуршког факултета, ангажовањем на пројекту Министарства просвете, науке и технолошког развоја под бројем ИИИ 46010 „Развој нових инкапсулационих ензимских технологија за производњу биокатализатора и биолошки активних компонената хране у циљу повећања њене конкурентности, квалитета и безбедности“. Од 1. маја 2018. запослена је у Центру за физику чвртог стања и нове материјале Института за физику у Београду као истраживач сарадник, у оквиру истог пројекта. У досадашњој каријери публиковала је три научна чланка од којих два категорије М21 и један категорије М22. Радови су до сада цитирани седам пута.

Преглед научне активности

Јасмина Ј. Лазаревић, дипломирани фармацеут, научно-истраживачки рад започела је 2013. године у Иновационом центру Технолошко-металуршког факултета Универзитета у Београду у оквиру пројекта под бројем ИИИИ 46010, под руководством проф. др Бранка Бугарског (сада проф. др Зорице Кнежевић-Југовић). Од 2018. активност је настављена у Институту за физику у Београду. Од самог почетка, кандидат се оријентисала ка Рамановој спектроскопији, као једној од моћних аналитичких метода данашњице, са акцентом на примени на фармаколошким/биолошким системима.

У оквиру докторских студија, положила је 12/12 испита предвиђених планом и програмом, са просечном оценом 10.00 и освојених 81 ЕСПБ. Октобра 2014. године одбранила је Завршни испит под називом „Развијање инструменталне методе-вибрационе спектроскопије у циљу идентификације биокатализатора“ пред Комисијом у саставу: др Бранко Бугарски, редовни професор Технолошко-металуршког факултета у Београду, др Зорица Кнежевић-Југовић, редовни професор Технолошко-металуршког факултета и др Рада Пјановић, ванредни професор Технолошко-металуршког факултета.

Област научно-истраживачког рада Јасмине Ј. Лазаревић је примена вибрационе спектроскопије, а посебно Раманове спектроскопије, у анализи фармаколошки активних супстанци и биолошких/биотехнолошких узорака. Досадашња научна активност може се поделити у две целине:

1. Полиморфизам фармацеутски активних једињења

Полиморфизам је особина чврстих супстанци да постоје у два или више кристалних облика, тј. да могу имати различите групе симетрије. Сматра се да више од 50% фармаколошки активних супстанци (и ексципијенаса) постоји у више од једног кристалног облика. Последице полиморфизма су различите физичко-хемијске карактеристике, као што су растворљивост, физичка и хемијска стабилност, хигроскопност итд. То се директно одражава како на технолошки поступак израде фармацеутског облика, тако и на последичну биорасположивост и фармакодинамику. Из тог разлога је неопходно извршити адекватну карактеризацију фармаколошки активне супстанце још у преформулативној фази. Познато је да код различитих полиморфних облика може доћи до малих промена положаја и/или интензитета раманских мода у високоенергетском делу спектра, који представља интрамолекулске вибрације, а услед пертурбације електронске структуре молекула окружењем. Међутим, на примеру ибупрофена, фокусирали смо се на нискоенергетски део Рамановог спектра, где очекујемо појаву вибрационих мода услед интермолекулских интеракција које су у директној вези са кристалном структуром. У оквиру ове активности до сада је објављен један научни чланак:

- **Lazarević J.J., Uskoković-Marković S., Jelikić-Stankov M., Radonjić M., Tanasković D., Lazarević N., Popović Z.V.:** *Intermolecular and low-frequency intramolecular Raman scattering study of racemic ibuprofen*, -Spectrochimica Acta Part A: Molecular and Biomolecular Spectroscopy, Vol 126, 2014, pp 301–305. (M22, IF 2014=2.353, ISSN=1386-1425)

2. Мезенхималне матичне ћелије – Фиксација и диференцијација

Ћелије и ткива поседују специфичне динамичке биохемијске маркере и молекулску структуру. Оптичка спектроскопија, која повезује биохемијски састав, молекулску структуру и њихове варијације, са дијагнозама различитих болести и поремећаја, била би веома моћно клиничко средство. Способност да истовремено детектује молекулске вибрације свих конституената без додатних обележивача, недеструктивност (посебно важна код испитивања ћелија и ткива), као и могућност мапирања са микронском латералном резолуцијом, чини Раманову спектроскопију одличним кандидатом. У ери развоја регенеративне медицине, матичне ћелије су од пресудног значаја. Употребили смо ову аналитичку методу у испитивању диференцијационог статуса примарних мезенхимских матичних ћелија пореклом из периодонталног лигамента, васкуларизоване везивне ткивне структуре које повезује корен зуба за алвеоларну кост. Матичне ћелије, стимулисане да диференцирају одређено време ка остеогеној, хондрогеној и адипогеној лози, фиксирани су и анализиране. Висока цена специјалних супстрата представља једну од великих препрека за имплементацију методе. С тим у вези, карактеризација је вршена на широко доступном супстрату-стаклу. Оно се карактерише значајном фотолуминесценцијом која утиче на спектар и тај утицај је умањен/елиминисан током обраде података. Други део истраживања матичних ћелија заснива се на испитивању утицаја хемијских фиксатива различитог механизма дејства на раманске спектре, будући да се највећи проценат испитивања, и у истраживачким и клиничким условима, врши на фиксираним ћелијама. Ради елиминације ометајућих фактора, као што је фотолуминесценција супстрата, мерење је вршено на плочицама калцијум-флуорида раманског степена чистоће.

Сви узорци матичних ћелија из периодонталног лигамента обезбеђени су од стране Групе за хематологију Института за медицинска истраживања Универзитета у Београду, а сви експерименти Рамановог расејања вршени су у Центру за физику чврстог стања и нове материјале Института за физику.

У оквиру ове научне активности објављени су следећи научни чланци:

- **Lazarević J.J.,** Kukolj T., Bugarski D., Lazarević N., Bugarski B., Popović Z.V.: *Probing primary mesenchymal stem cells differentiation status by micro-Raman spectroscopy*, - Spectrochimica Acta Part A: Molecular and Biomolecular Spectroscopy, Vol 213, 2019, pp 384–390. (M21, IF 2017=2.880, ISSN=1386-1425)
- **Lazarević J.J.,** Ralević U., Kukolj T., Bugarski D., Lazarević N., Bugarski B., Popović Z.V.: *Influence of chemical fixation process on primary mesenchymal stem cells evidenced by Raman spectroscopy*, Spectrochimica Acta Part A: Molecular and Biomolecular Spectroscopy, Vol 216, 2019, pp 173-178. (M21, IF 2017=2.880, ISSN=1386-1425)

Објављени научни радови и саопштења Јасмине Лазаревић:

Рад у врхунском међународном часопису (M21)

- **Lazarević J.J.**, Kukolj T., Bugarski D., Lazarević N., Bugarski B., Popović Z.V.: *Probing primary mesenchymal stem cells differentiation status by micro-Raman spectroscopy*, - Spectrochimica Acta Part A: Molecular and Biomolecular Spectroscopy, Vol 213, 2019, pp 384–390. (IF 2017=2.880, ISSN=1386-1425)
- **Lazarević J.J.**, Ralević U., Kukolj T., Bugarski D., Lazarević N., Bugarski B., Popović Z.V.: *Influence of chemical fixation process on primary mesenchymal stem cells evidenced by Raman spectroscopy*, Spectrochimica Acta Part A: Molecular and Biomolecular Spectroscopy, Vol 216, 2019, pp 173-178. (IF 2017=2.880, ISSN=1386-1425)

Рад у истакнутом међународном часопису (M22)

- **Lazarević J.J.**, Uskoković-Marković S., Jelikić-Stankov M., Radonjić M., Tanasković D., Lazarević N., Popović Z.V.: *Intermolecular and low-frequency intramolecular Raman scattering study of racemic ibuprofen*, -Spectrochimica Acta Part A: Molecular and Biomolecular Spectroscopy, Vol 126, 2014, pp 301–305. (IF 2014=2.353, ISSN=1386-1425)

Саопштење на међународном скупу штампано у изводу (M34)

- **Lazarević Jasmina J.**, Kukolj Tamara, Bugarski Diana, Lazarević Nenad, Popović Zoran V. and Bugarski Branko, Fourteenth Young Research Conference - Material Sciece and Engineering: Program and Book of Abstracts, 2015, 6, isbn: 978-86-80321-31-8.

1-5

Probing mesenchymal stem cells differentiation status by micro Raman spectroscopy

Jasmina J. Lazarević,¹ Tamara Kukolj,² Diana Bugarski,² Nenad Lazarević,³
Zoran V. Popović,³ and Branko Bugarski⁴

¹*Innovation center, Faculty of Technology and Metallurgy, University of Belgrade, Karnegijeva 4, 11060 Belgrade, Serbia,* ²*Laboratory for Experimental Hematology and Stem Cells, Institute for Medical Research, University of Belgrade, 11000 Belgrade, Serbia,* ³*Center for Solid State Physics and New Materials, Institute of Physics Belgrade, University of Belgrade, Pregrevica 118, 11080 Belgrade, Serbia,* ⁴*Department of Chemical Engineering, Faculty of Technology and Metallurgy, University of Belgrade, Karnegijeva 4, 11060 Belgrade, Serbia*

The main goal of tissue engineering, a rapidly growing field in regenerative medicine, is to cultivate tissues and organs in vitro that can be used as transplantation grafts. The leading role in this area belongs to stem cells due to their unique potential to differentiate into various cell types. However, suitable analytical tools for stem cell differentiation capacity and homogeneity investigation are still to be defined (and improved). Micro Raman spectroscopy is non-destructive and non-invasive optical technique, which requires neither sample preparation nor exogenous labels that can affect chemistry of the sample. Owing to this features, it might be a potential method of choice for biological samples. The focus of this research was on multilineage differentiation potential of human mesenchymal stem cells isolated from periodontal ligament. These cells were stimulated to osteogenic, adipogenic, and chondrogenic differentiation. We used micro Raman spectroscopy as a tool for probing inner cell structure and assessing the differentiation status. The difference between spectra obtained from undifferentiated and differentiated cells has been observed. Moreover, a comprehensive statistical analysis has been performed.



Contents lists available at ScienceDirect

Spectrochimica Acta Part A: Molecular and Biomolecular Spectroscopy

journal homepage: www.elsevier.com/locate/saa

Influence of chemical fixation process on primary mesenchymal stem cells evidenced by Raman spectroscopy

J.J. Lazarević^a, U. Ralević^a, T. Kukolj^b, D. Bugarski^b, N. Lazarević^{a,*}, B. Bugarski^c, Z.V. Popović^{a,d}

^aCenter for Solid State Physics and New Materials, Institute of Physics Belgrade, University of Belgrade, Pregrevica 118, Belgrade 11080, Serbia

^bLaboratory for Experimental Hematology and Stem Cells, Institute for Medical Research, University of Belgrade, Belgrade 11000, Serbia

^cDepartment of Chemical Engineering, Faculty of Technology and Metallurgy, University of Belgrade, Karnegijeva 4, Belgrade 11060, Serbia

^dSerbian Academy of Sciences and Arts, Knez Mihailova 35, Belgrade 11000, Serbia

ARTICLE INFO

Article history:

Received 7 December 2018

Received in revised form 6 March 2019

Accepted 6 March 2019

Available online 9 March 2019

Keywords:

Raman spectroscopy

Stem cells

Chemical fixation

ABSTRACT

In investigation of (patho)physiological processes, cells represent frequently used analyte as an exceptional source of information. However, spectroscopic analysis of live cells is still very seldom in clinics, as well as in research studies. Among others, the reasons are long acquisition time during which autolysis process is activated, necessity of specified technical equipment, and inability to perform analysis in a moment of sample preparation. Hence, an optimal method of preserving cells in the existing state is of extreme importance, having in mind that selection of fixative is cell lineage dependent. In this study, two commonly used chemical fixatives, formaldehyde and methanol, are used for preserving primary mesenchymal stem cells extracted from periodontal ligament, which are valuable cell source for reconstructive dentistry. By means of Raman spectroscopy, cell samples were probed and the impact of these fixatives on their Raman response was analyzed and compared. Different chemical mechanisms are the core processes of formaldehyde and methanol fixation and certain Raman bands are shifted and/or of changed intensity when Raman spectra of cells fixed in that manner are compared. In order to get clearer picture, comprehensive statistical analysis was performed.

© 2019 Elsevier B.V. All rights reserved.

1. Introduction

Mesenchymal stem cells (MSCs) are heterogenous group of adult stem cells originally discovered in bone marrow, but present in all tissues and organs, with the purpose to keep tissue homeostasis, regeneration and renewal. These acts are performed not only through multipotent differentiation potential (toward chondrogenic, adipogenic, and osteogenic lineages), but also through their ability to modulate immune response (directly or indirectly) [1–5]. Although MSCs possess common cellular features, it is overall accepted that these cells still exhibit variable regenerative capacity due to different tissue origin, donor diversity, and variations in culture conditions [6,7]. Human MSCs investigated in this study originate from periodontal ligament, a fibrous, cellular, and vascular soft connective tissue. The main role of periodontal ligament is to anchor tooth to the alveolar bone, maintain mineralisation level and alleviate mechanical forces associated with the process of mastication [8–10]. Previously, it was demonstrated that human periodontal ligament

stem cells (hPDLSCs) investigated in this experiment fulfill criteria for MSCs identification and characterization, set by The International Society for Cell Therapy (ISCT) [11,12]. Minimal criteria for characterization of human MSCs, set by ISCT, include plastic adhesion, with expression of CD73, CD90, CD105 surface markers and lack of hematopoietic markers CD34–, CD45–, CD14–, CD79 α –, HLA-DR–; and multilineage differentiation potential into osteoblasts, adipocytes, and chondroblasts [13]. However, MSCs nature, including hPDLSCs, is still elusive. Therefore, the exploration of hPDLSCs, as a cell source for reconstructive dentistry, is of great importance for the novel therapeutic strategies related to recovery of periodontium and curing dental defects [14].

Taking into account the heterogeneity of MSCs, it is crucial for these cells to be adequately characterized during the lifespan, before further manipulation. Although many techniques are available in this field, including mass spectroscopy, flow cytometry, and immunocytochemistry, most of them are destructive, invasive, time consuming or require expensive cell-specific labels [15,16]. However, a light scattering technique, Raman spectroscopy, is able to overrun these issues due to its unique properties: it is non-invasive, non-destructive, fast, label-free, and complex sample preparation is not required. It operates with low sample volume even in aqueous

* Corresponding author.

E-mail address: nenadl@ipb.ac.rs (N. Lazarević).

solutions and provide a plenty of biochemical information as an outcome. Raman spectroscopy is a type of vibrational spectroscopy, based on Raman effect [17], in which an inelastically scattered component of the visible light bears the information of the analyte. Raman scattering experiment results in vibrational spectrum, a fingerprint of a sample, which carries the information about chemical composition and structure of a sample, on a submolecular level. Typically, it comprises vibrational modes of the highest Raman scattering cross section [16, 18–20].

Spectroscopic analysis of live cells is still very seldom, both in clinical and research conditions, particularly due to the longevity of the processes, when autolysis is inevitable. On the other hand, it is not always possible to investigate a sample in a moment of acquiring. The crucial and fundamental step in cell biology, for obtaining sensitive and reproducible results, is a process called fixation, which maintain the localization of biomolecules. It is used for preserving a cell in a physiological state, by preventing cell shrinkage or swelling caused by osmotic pressure initiated with air-drying, as well as autolysis by activating lysosomal enzymes, which includes denaturation of proteins, dephosphorylation of mononucleotides, phospholipids and proteins, chromatin compaction, nuclear fragmentation, and cytoplasmic condensation and fragmentation [21]. However, it is known that selection of a fixative is very much dependent on a cell nature when it comes to Raman spectroscopy and can significantly distort experimental data [22]. In the past decade, investigations of different fixatives' influence on Raman spectra of numerous cell lineages were reported, with an aim to clarify the best option for each cell lineage. One of the studies investigated the effect of formaldehyde and ethanol fixation on CARS (Coherent Anti-Stokes Raman Spectroscopy) signal of proteins and lipids in different cellular compartments of glial and neuronal cells, concluding that formaldehyde fixation is preferable method of preservation of these cells [22]. Also, the effect of chemical fixation procedures on the Raman spectra of normal and leukemia cells was characterized [23]. When compared to the spectra of unfixed cells, the fixed cell spectra showed changes in the intensity of specific Raman markers, and latter statistical analysis suggested that methanol provokes greater changes in Raman spectra when compared to paraformaldehyde. Further, micro-Raman spectroscopy was employed for chemical fixation mechanism study in three cell lines (normal skin, normal bronchial epithelium, and lung adenocarcinoma) [24]. Nucleic acid degradation, protein denaturation, and lipid leaching was observed with all fixatives (formalin, Carnoy's fixative, and methanol-acetic acid) and for all cell lines, but to varying degrees. Also, the authors suggested that formalin best preserves cellular integrity and gives the closest spectral content to that in live cells. The next study monitored the impact of fixation by formalin, desiccation, and air-drying on *in vitro* cell culture lines [25]. The results indicate that the choice of fixation methodology significantly influences the quality and reproducibility of the resulting spectral data. Formalin showed inconsistency in sample preservation and a loss of signal intensity, while air-drying appears to be inconsistent in terms of spectral reproducibility. Desiccation showed good spectral reproducibility and good signal-to-noise ratio [25].

Although numerous Raman studies of fixative process' spectral influence have been performed [22–25], according to our knowledge, no such research has been performed on primary mesenchymal stem cells originating from periodontal ligament. We used micro-Raman spectroscopy in order to probe fixed hPDLSCs and investigate the effects of two most frequently used chemical fixatives which have different chemical mechanisms of preservation (formaldehyde and methanol), and then compared those effects. Formaldehyde reacts extensively with amino groups to form methylene bridges and cross-links molecules, which alters, but stabilizes them [26]. Further, formaldehyde does not appear to perturb tertiary structure very much. On the other hand, methanol replaces water in cell environment, disrupts hydrophobic and hydrogen bonding, and

consequently alters tertiary structure of proteins [27,28]. Although fixation substantially alters composition and appearance, it is possible to produce consistent chemical and physical properties by selection of suitable preparation conditions. Nevertheless, standardization of Raman spectroscopy regarding fixative selection could provide valuable additional information in many biological tests that require cell fixation and also indicate the existence of fine differences in the fixative effect that are necessary to be taken into consideration during standard biological protocols.

2. Experiment

2.1. Isolation and Cultivation of Human Periodontal Ligament Stem Cells

After getting the informed consent from healthy patients (age 18), subjected to the procedure of tooth extraction for orthodontic reasons, at the Department of Oral Surgery of the Faculty of Dental Medicine, the University of Belgrade, human periodontal ligament tissues from normal impacted third molars were collected. Immediately after, tissues were placed in sterile cell culturing conditions. As previously reported [11], human PDLSCs were isolated, characterized and expanded. For hPDLSCs isolation, periodontal tissues were carefully detached from the mid-third of the root surface, cut into small pieces and placed in a 25 cm² flask with Dulbecco's modified Eagle's medium (DMEM; Sigma-Aldrich St. Louis, MO, USA) supplemented with 10% fetal bovine serum (FBS; Capricorn-Scientific, Germany), 100 U/ml penicillin and 100 mg/ml streptomycin (Gibco, Thermo Fisher Scientific, USA). Standard cultivation conditions included 37 °C temperature, humidified atmosphere containing 5% CO₂, while medium was exchanged two times per week. After reaching 80% to 90% confluence, cells were detached regularly in growth medium (GM-DMEM with 10% FBS) using 0.05% trypsin with 1 mM EDTA (Gibco, Thermo Fisher Scientific, USA). In order to demonstrate the universality of experimental results for MSCs, cells from third and sixth passages were used, divided into two batches. Moreover, hPDLSCs were characterized based on immunophenotype and multipotent differentiation potential toward osteogenic, chondrogenic and adipogenic lineages as it has been described before [11]. All treatments were performed according to the approved ethical guidelines set by Ethics Committee of the Faculty of Dental Medicine, University of Belgrade and Declaration of Helsinki.

2.2. Sample Preparation

For the Raman experiment, hPDLSCs were seeded on rounded CaF₂ slides in 24-well plate (5 × 10³ cells per slide) and cultivated in GM in standard cultivation conditions during 24 h. Following the adhesion, hPDLSCs were washed with saline buffer and fixed with 3.7% formaldehyde or methanol for 10 min at room temperature. Right before Raman spectroscopy was performed, samples were washed with distilled water.

2.3. μ -Raman Spectroscopy

In most of the cases, the Raman spectroscopy independently probes single vibrations within a molecule or a crystal, but in a complex biological systems composed of various types of macromolecules, only vibrational bands consisting of numerous vibrations of the same type, rather than a single vibration, could be distinguished. Consequently, the changes of biological system composition may result with a change of certain Raman bands line-shapes and/or intensities.

The Raman scattering experiment was performed using NTegra Spectra from NTMDT. The 532 nm line of a semiconductor laser was used as an excitation source. The laser power was set to 2 mW

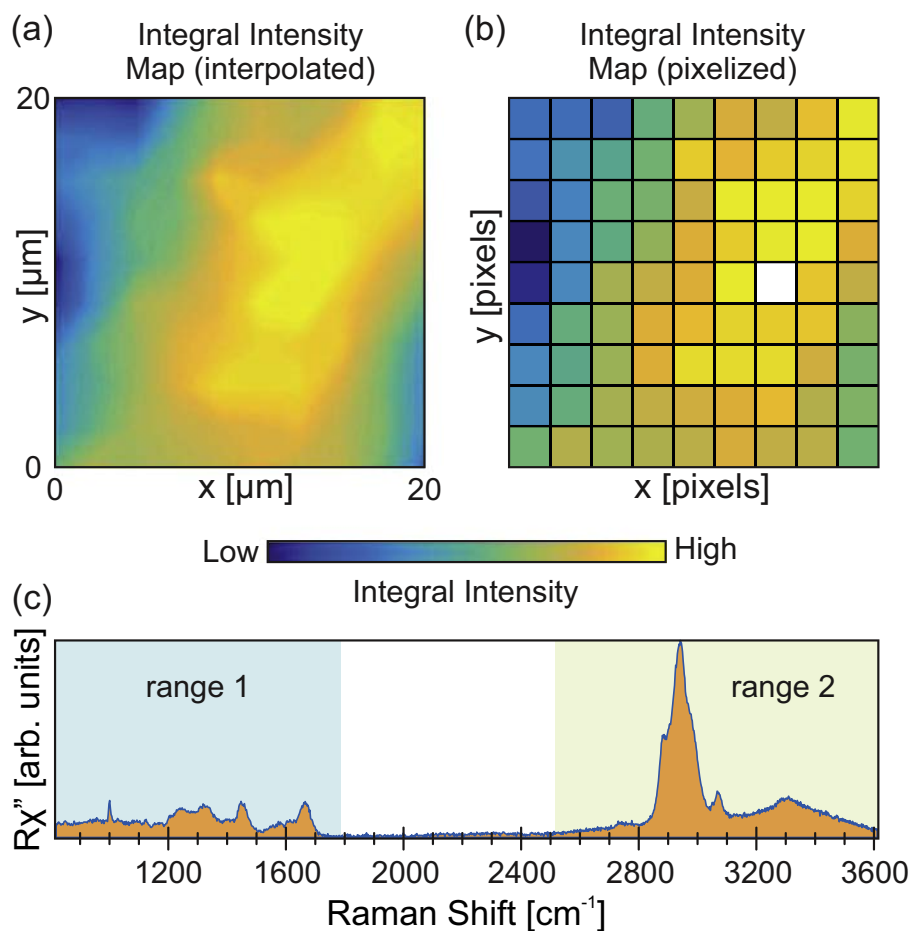


Fig. 1. A single PDLSC Raman (a) interpolated integral intensity map, and (b) pixelized integral intensity map. (c) Human PDLSC Raman scattering spectrum acquired on a pixel marked in white.

and focused on the area of about $1\ \mu\text{m}$, in order to provide a reasonable Raman intensity for a 60 s long acquisition. Under these conditions, the sample associated Raman bands, acquired sequentially at the same position, were found to be stable in terms of both the band intensity and spectral position. In other words, no visible laser induced modifications of the cells were observed upon repeating the signal acquisition for a few times at any of the acquisition points.

Due to very complex inner structure of a cell, there may be small variations in Raman spectra for the data collected at different positions. Consequently, suitable methodology must be applied in order to achieve the needed level of sample representation. In other words, the applied method has to be robust. Here, two batches of cells treated with methanol and formaldehyde were examined by spatially mapping the Raman scattering signal on 20 cells per batch. The spectra were collected at 10×10 or 11×11 matrices of spatial points separated by a distance larger than the estimated focus diameter of $\approx 1\ \mu\text{m}$. The distance between adjacent spatial points, or the spatial resolution, was varied between $2\ \mu\text{m}$ and $3\ \mu\text{m}$ depending on the cell size. The example of an interpolated spectral map of a single methanol fixed cell is presented in Fig. 1(a). Fig. 1(b) shows the same map with the actual pixels omitting the interpolation for clarity. The x and y represent spatial coordinates in which a spectrum is acquired. The intensity of a pixel, labeled white in Fig. 1(b), is obtained by integrating the Raman spectra collected at that pixel. The value of the integral is equal to the area below the acquired signal as illustrated by shaded (orange) area below the typical hPDLSC

Raman spectra in Fig. 1(c). It is characterized by clearly visible Raman bands in two spectral regions marked in Fig. 1(c). The first spectral region spans from $800\ \text{cm}^{-1}$ to $1770\ \text{cm}^{-1}$, whereas the second starts at $2500\ \text{cm}^{-1}$ and ends at $3600\ \text{cm}^{-1}$.

2.4. Data Processing and Analysis

In addition to typical PDLSCs Raman spectra [Fig. 1(c)], a few (in total) significantly different spectra, having an extremely high

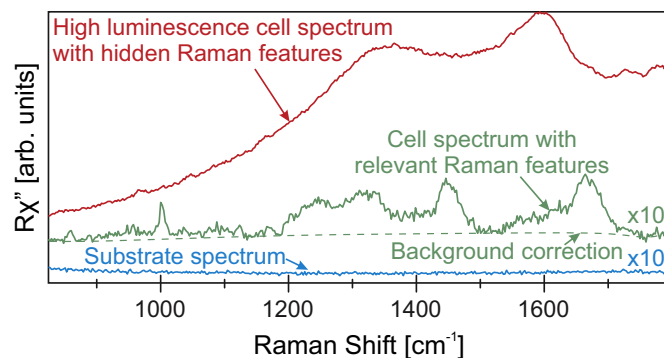


Fig. 2. A typical PDLSCs, substrate, and high luminescence points Raman spectra in the range from $800\ \text{cm}^{-1}$ to $1800\ \text{cm}^{-1}$, depicting spectral selection and preprocessing.

luminescence contribution, were observed as well. The example of such a spectrum truncated to the spectral region from 800 cm^{-1} to 1770 cm^{-1} is shown in Fig. 2. Clearly, extremely strong luminescence masks the relevant Raman bands, making them misleading. Consequently, the high luminescence spectra were omitted from the analysis. The relevant Raman spectra were preprocessed before further manipulation. In the initial step, the background, modelled as a polynomial function of the fourth degree, was subtracted (see Fig. 2). Upon background removal, the spectra were normalized to the value of the integral intensity, calculated within the considered spectral region and then subjected to the analysis.

Besides the direct comparison of the Raman spectra of the cells fixed with formaldehyde and methanol, a multivariate statistical method, principal component analysis (PCA), was applied [15,18,29,30]. Thereby, the dimensionality of the experimental data set is reduced, by transforming to a new set of variables, the principal components, which are uncorrelated and ordered in a way that the first few retain most of the variation present in all of the original variables [31]. The outcome of this analysis is distinct grouping of Raman spectra based on their mutual features [18,29].

3. Results and Discussion

Regarding biological background of our samples, it is well known that primary mesenchymal stem cell cultures represent heterogenic cellular populations, thus the intrinsic heterogeneity of primary cells should be taken into consideration. Moreover, cellular features of

these cells are highly prone to modifications during standard cultivation process [32,33]. Therefore, in order to get reproducible results, we analyzed cells from different passages (passage 3 in Batch 1 and passage 6 in Batch 2).

It is known that the effect of fixation process is cell type and fixative dependent [25]. Different chemical mechanisms may result in variations of the respective Raman spectra. Whereas depletion of certain component will result in reduction of corresponding Raman bands' intensities, various perturbations of the electronic cloud will lead to the changes of bands energy and linewidth. The second does not exclude the possibility of variations of the Raman intensities since the change in electronic structure may impact probability of the inelastic light scattering processes. In our data, the most pronounced changes are occurring in two spectral regions [Fig. 1], ranging from 800 cm^{-1} to 1770 cm^{-1} and from 2500 cm^{-1} to 3600 cm^{-1} . In the statistical treatment, these regions were analyzed independently due to the intrinsic imperfections of the spectrometer.

In Fig. 3, 2D Raman spectra map, averaged spectra, their difference and PCA of Batch 1 and Batch 2 of formaldehyde and methanol fixed PDLSCs, are presented respectively, for spectral region between 800 cm^{-1} and 1770 cm^{-1} . Closer inspection of formaldehyde and methanol fixed PDLSCs 2D Raman spectra map [Fig. 3(a) and (c)] already reveals significant difference between two groups. Relative change of intensity and/or energy shift can be clearly observed for multiple Raman bands. This is even more evident in the difference of formaldehyde and methanol fixed PDLSCs average Raman spectra [Fig. 3(a) and (c)]. It can be seen that phenylalanine peaks at 1002 cm^{-1} and 1030 cm^{-1} are of higher intensity in methanol fixed PDLSCs Raman spectra compared to formaldehyde fixed ones.

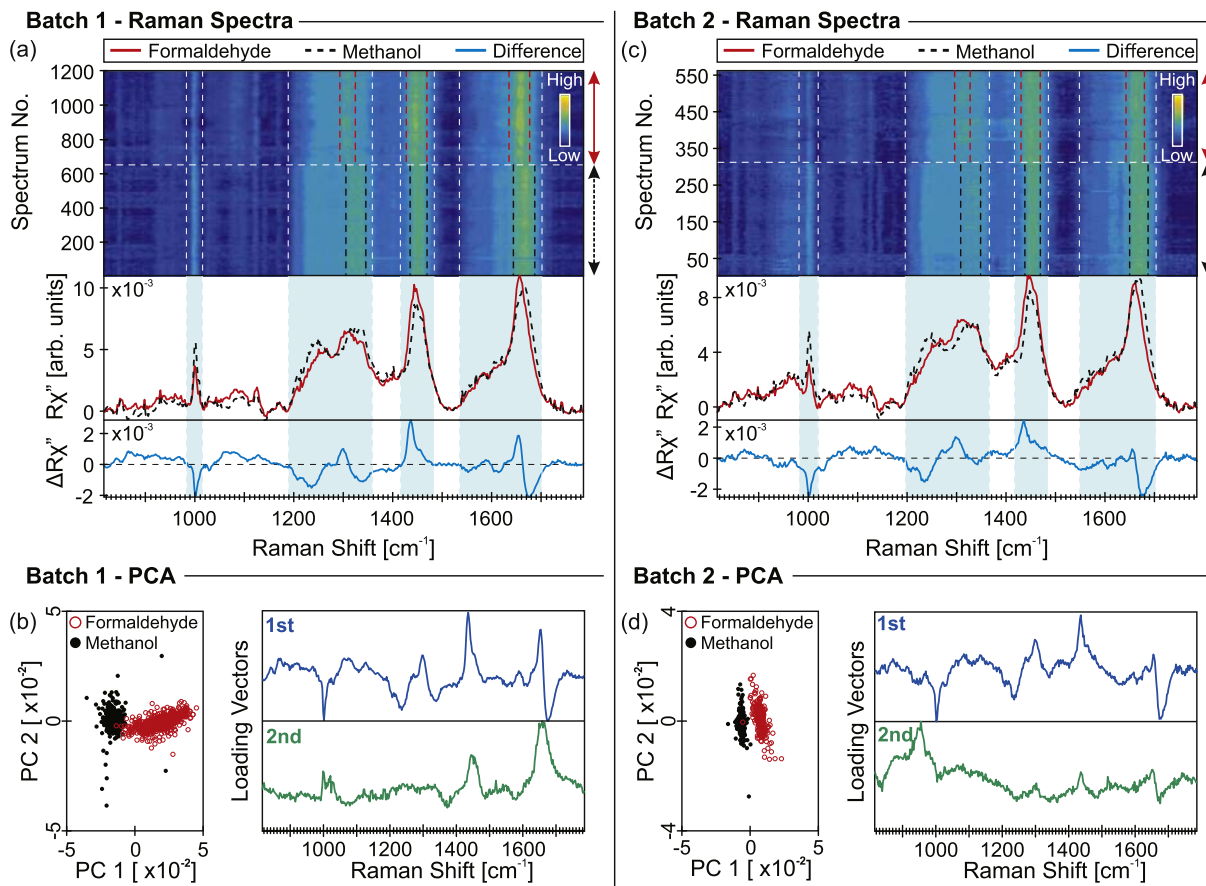


Fig. 3. 2D Raman spectra map obtained from PDLSCs (see Supplementary information), fixed with formaldehyde and methanol, their mean spectra, as well as their difference for the spectral region from 800 cm^{-1} to 1770 cm^{-1} ; PCA score plots calculated for these two groups of cells, and PCA loading vectors for (a)–(b) Batch 1 and (c)–(d) Batch 2, respectively. Percentage of variance PC1–PC2: for Batch 1 19.85%–5.76%; for Batch 2 17.95%–7.43%.

The DNA bands at 1095 cm^{-1} , 1130 cm^{-1} , and 1330 cm^{-1} are of higher intensity in formaldehyde fixed PDLSCs spectra whereas the band at about 1330 cm^{-1} is also slightly shifted. Amide III band at about 1260 cm^{-1} is significantly shifted and of higher intensity in methanol fixed spectra. When it comes to lipid band at 1450 cm^{-1} , it is of noticeable higher intensity and shifted in formaldehyde fixed spectra, as well as the Amide I band at about 1660 cm^{-1} .

The observed behaviour is consistent with the biochemical picture in which the protein content is larger in methanol fixed cells. This is evidenced by more pronounced phenylalanine peak. On the other hand, the secondary structure is more preserved in formaldehyde fixed samples (Amide I band). Modification of native proteins by formaldehyde does not perturb the secondary structure very much. Lipid content is maintained greatly in formaldehyde fixed sample, which is in a good agreement with the literature, due to methanol-caused leaching of lipids through deteriorated cell membrane. As a consequence of cross-linking mechanism of fixation, DNA level is maintained in greater moiety in formaldehyde fixed PDLSCs Raman spectrum [27,28,34].

Spectra of averaged formaldehyde and methanol fixed PDLSCs spectra, and their difference spectrum, from Batch 2 are given in Fig. 3(c). The only observable difference, in comparison to Batch 1, is lower intensity of Amide I band at 1660 cm^{-1} in formaldehyde fixed PDLSCs Raman spectrum, relative to methanol fixed PDLSCs spectrum.

The same procedure is repeated for spectral region from 2500 cm^{-1} to 3600 cm^{-1} . In Fig. 4, 2D Raman spectra map, averaged

spectra, their difference, and PCA of Batch 1 and Batch 2 of formaldehyde and methanol fixed PDLSCs, are presented respectively. Again, formaldehyde and methanol fixed PDLSCs Raman spectra are compared in this spectral region which reflects protein, lipid, and water content. In Fig. 4(a) and (c), it is observable from averaged spectra of difference that the bands at 2860 cm^{-1} and 2890 cm^{-1} , are more intense in formaldehyde fixed PDLSCs Raman spectra. These two bands present CH_2 and CH_3 symmetric stretch in lipids and proteins [35]. Raman band at 2940 cm^{-1} is assigned to CH vibrations in lipids and proteins and is more pronounced in methanol fixed PDLSCs Raman spectra. This confirms above-mentioned statements that formaldehyde better maintains the level of lipids with regard to methanol. On the other hand, methanol keeps protein levels.

Further, PCA is applied for the treatment of the spectral data, and the outcome is presented in Figs. 3 (b), (d) and 4(b), (d) for Batch 1 and Batch 2, respectively. Analyzing PCA score plots, clear assemblage of cells fixed with the same fixative is observable and, as expected, in all cases, PC1 is the component that makes the difference [Figs. 3(b), (d), and 4(b), (d)]. Only a few overlapping points have been observed due to the heterogeneity of the samples and/or variable signal-to-noise ratio. For illustration, PC2s and corresponding loading vectors are also presented. They represent intra- and inter-cellular variations, within the group of cells fixed with the same fixative. PC1 loading vectors are consistent with discrepancies directly observable in Raman spectra of differences, as discussed above. This is not surprising, having in mind the nature of this principal component and the algorithms applied.

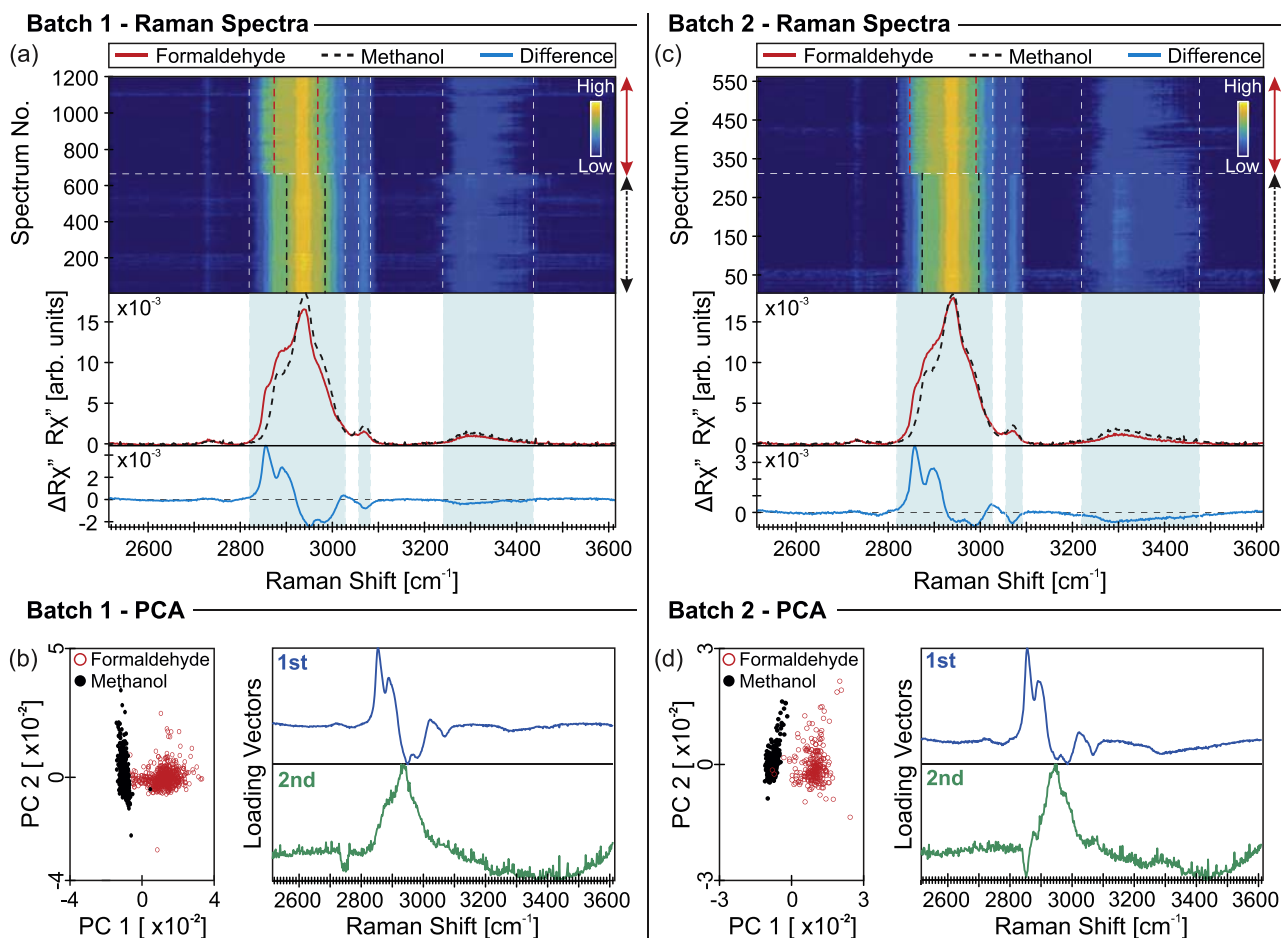


Fig. 4. 2D Raman spectra map obtained from PDLSs (see Supplementary information), fixed with formaldehyde and methanol, their mean spectra, as well as their difference for spectral region from 2500 cm^{-1} to 3600 cm^{-1} ; PCA score plots calculated for these two groups of cells, and PCA loading vectors for (a)–(b) Batch 1 and (c)–(d) Batch 2, respectively. Percentage of variance PC1–PC2: for Batch 1 64.09%–12.59%; for Batch 2 60.08%–14.64%.

Closer inspection of PCA score plots [Figs. 3(b), (d), and 4(b), (d)] reveals greater spread along PC1 for Batch 1, in particular for the spectral region from 800 cm⁻¹ to 1770 cm⁻¹ of formaldehyde fixed cells. This is most likely a consequence of heterogeneity of these primary cells. Depending on the nature of the inter-/intracellular variations, fixation process may enhance and/or suppress their Raman spectra signatures [22–26]. Detailed comparison between batches for both fixatives is presented in the Supplementary information.

4. Conclusion

Fixatives cause dramatic changes for all cell types but to varying extent. It is crucial to have a clear idea of what is expected from the sample when choosing the fixative agent. Preservation of cells by formaldehyde and methanol treatment represents standard procedures in most laboratory protocols. In this study, we investigated the effects of these two chemicals on Raman spectra of primary cell lineage, PDLSCs. Both procedures provided quantitatively and qualitatively close Raman spectra that can be considered as fingerprint spectra for this cell lineage. Through the direct comparison of the Raman spectra, as well as the statistical treatment, subtle differences have been observed between two groups that can be traced back to the variations in lipid and protein content. Consequently, when choosing the fixation method, the purpose of investigation has to be kept in mind. When it comes to Raman spectroscopy of hPDLSCs, both formaldehyde and methanol are acceptable choices, but with unlike sensitivity for tracing different biochemical composition.

Acknowledgments

We gratefully acknowledge M. Miletić and M. Andrić for supplying the periodontal ligament tissue. This work was supported by the Ministry of Education, Science, and Technological Development of the Republic of Serbia under Projects Nos. III46010, III45018, ON175062, and OI171005.

Appendix A. Supplementary Data

Supplementary data to this article can be found online at <https://doi.org/10.1016/j.saa.2019.03.012>.

References

- [1] M. Gazdic, V. Volarevic, N. Arsenijevic, M. Stojkovic, Mesenchymal stem cells: a friend or foe in immune-mediated diseases, *Stem Cell Rev. Rep.* 11 (2) (2015) 280–287.
- [2] Y. Sato, H. Araki, J. Kato, K. Nakamura, Y. Kawano, M. Kobune, T. Sato, K. Miyayoshi, T. Takayama, M. Takahashi, et al. Human mesenchymal stem cells xenografted directly to rat liver are differentiated into human hepatocytes without fusion, *Blood* 106 (2) (2005) 756–763.
- [3] R.O. Oreffo, C. Cooper, C. Mason, M. Clements, Mesenchymal stem cells, *Stem Cell Rev.* 1 (2) (2005) 169–178.
- [4] A.R. Williams, J.M. Hare, Mesenchymal stem cells biology, pathophysiology, translational findings, and therapeutic implications for cardiac disease, *Circ. Res.* 109 (8) (2011) 923–940.
- [5] J. Lazarević, T. Kukulj, D. Bugarski, N. Lazarević, B. Bugarski, Z. Popović, Probing primary mesenchymal stem cells differentiation status by micro-Raman spectroscopy, *Spectrochim. Acta A Mol. Biomol. Spectrosc.* 213, 384–390.
- [6] R. Hass, C. Kasper, S. Böhm, R. Jacobs, Different populations and sources of human mesenchymal stem cells (msc): a comparison of adult and neonatal tissue-derived msc, *Cell Commun. Signal* 9 (1) (2011) 12.
- [7] D.G. Phinney, Functional heterogeneity of mesenchymal stem cells: implications for cell therapy, *J. Cell. Biochem.* 113 (9) (2012) 2806–2812.
- [8] I.C. Gay, S. Chen, M. MacDougall, Isolation and characterization of multipotent human periodontal ligament stem cells, *Orthod. Craniofacial Res.* 10 (3) (2007) 149–160.
- [9] S. Ivanovski, S. Gronthos, S. Shi, P. Bartold, Stem cells in the periodontal ligament, *Oral Dis.* 12 (4) (2006) 358–363.
- [10] M. Shimono, T. Ishikawa, H. Ishikawa, H. Matsuzaki, S. Hashimoto, T. Muramatsu, K. Shima, K.I. Matsuzaka, T. Inoue, Regulatory mechanisms of periodontal regeneration, *Microsc. Res. Tech.* 60 (5) (2003) 491–502.
- [11] A. Miletić, S. Mojsilović, I. Okić-Djordjević, T. Kukulj, A. Jauković, J. Santibanez, G. Jovčić, D. Bugarski, Mesenchymal stem cells isolated from human periodontal ligament, *Arch. Biol. Sci.* 66 (1) (2014) 261–271.
- [12] T. Kukulj, D. Trivanović, I.O. Djordjević, J. Mojsilović, J. Krstić, H. Obradović, S. Janković, J.F. Santibanez, A. Jauković, D. Bugarski, Lipopolysaccharide can modify differentiation and immunomodulatory potential of periodontal ligament stem cells via ERK1, 2 signaling, *J. Cell. Physiol.* 233 (1) (2018) 447–462.
- [13] A. Klimczak, U. Kozłowska, Mesenchymal stromal cells and tissue-specific progenitor cells: their role in tissue homeostasis, *Stem Cells Int.* 2016 (2016) 1–11.
- [14] H. Egusa, W. Sonoyama, M. Nishimura, I. Atsuta, K. Akiyama, Stem cells in dentistry—part II: clinical applications, *J. Prosthodont. Res.* 56 (4) (2012) 229–248.
- [15] A. Downes, R. Mouras, A. Elfick, Optical spectroscopy for noninvasive monitoring of stem cell differentiation, *BioMed Res. Int.* 2010 (2010) 1–10.
- [16] A. Downes, R. Mouras, P. Bagnaninchi, A. Elfick, Raman spectroscopy and CARS microscopy of stem cells and their derivatives, *J. Raman Spectrosc.* 42 (10) (2011) 1864–1870.
- [17] C.V. Raman, K.S. Krishnan, A new type of secondary radiation, *Nature* 121 (3048) (1928) 501.
- [18] J.W. Chan, D.K. Lieu, Label-free biochemical characterization of stem cells using vibrational spectroscopy, *J. Biophotonics* 2 (11) (2009) 656–668.
- [19] A.F. Palonpon, J. Ando, H. Yamakoshi, K. Dodo, M. Sodeoka, S. Kawata, K. Fujita, Raman and SERS microscopy for molecular imaging of live cells, *Nat. Protoc.* 8 (4) (2013) 677–692.
- [20] I. Notingher, I. Bisson, A.E. Bishop, W.L. Randle, J.M. Polak, L.L. Hench, In situ spectral monitoring of mRNA translation in embryonic stem cells during differentiation in vitro, *Anal. Chem.* 76 (11) (2004) 3185–3193.
- [21] F. Lyng, E. Gazi, P. Gardner, Preparation of Tissues and Cells for Infrared and Raman Spectroscopy and Imaging, *Biomedical Applications of Synchrotron Infrared Microspectroscopy: A Practical Approach*, Royal Society of Chemistry, Cambridge, 2010, 147–191.
- [22] S.M. Levchenko, X. Peng, L. Liu, J. Qu, The impact of cell fixation on CARS signal intensity in neuronal and glial cell lines, *J. Biophotonics* (2018) e201800203.
- [23] J.W. Chan, D.S. Taylor, D.L. Thompson, The effect of cell fixation on the discrimination of normal and leukemia cells with laser tweezers Raman spectroscopy, *Biopolymers Original Res. Biomol.* 91 (2) (2009) 132–139.
- [24] A.D. Meade, C. Clarke, F. Draux, G.D. Sockalingum, M. Manfait, F.M. Lyng, H.J. Byrne, Studies of chemical fixation effects in human cell lines using Raman microspectroscopy, *Anal. Bioanal. Chem.* 396 (5) (2010) 1781–1791.
- [25] M.M. Mariani, P. Lampen, J. Popp, B.R. Wood, V. Deckert, Impact of fixation on in vitro cell culture lines monitored with Raman spectroscopy, *Analyst* 134 (6) (2009) 1154–1161.
- [26] E.A. Hoffman, B.L. Frey, L.M. Smith, D.T. Auble, Formaldehyde crosslinking: a tool for the study of chromatin complexes, *J. Biol. Chem.* (2015) jbc-R115.
- [27] M. Noguchi, J.S. Furuya, T. Takeuchi, S. Hirohashi, Modified formalin and methanol fixation methods for molecular biological and morphological analyses, *Pathol. Int.* 47 (10) (1997) 685–691.
- [28] J. Shaham, Y. Bomstein, A. Meltzer, Z. Kaufman, E. Palma, J. Ribak, DNA-protein crosslinks, a biomarker of exposure to formaldehyde-in vitro and in vivo studies, *Carcinogenesis* 17 (1) (1996) 121–126.
- [29] T. Ichimura, K.F. Liang-da Chiu, S. Kawata, T.M. Watanabe, T. Yanagida, H. Fujita, Visualizing cell state transition using Raman spectroscopy, *PLoS One* 9 (1) (2014) 1–8.
- [30] E. Brauchle, K. Schenke-Layland, Raman spectroscopy in biomedicine—non-invasive in vitro analysis of cells and extracellular matrix components in tissues, *Biotechnol. J.* 8 (3) (2013) 288–297.
- [31] I. Jolliffe, Principal component analysis, *International Encyclopedia of Statistical Science*, Springer, 2011, pp. 1094–1096.
- [32] W. Wagner, P. Horn, M. Castoldi, A. Diehlmann, S. Bork, R. Saffrich, V. Benes, J. Blake, S. Pfister, V. Eckstein, et al. Replicative senescence of mesenchymal stem cells: a continuous and organized process, *PLoS One* 3 (5) (2008) e2213.
- [33] Y.H.K. Yang, C.R. Ogando, C.W. See, T.Y. Chang, G.A. Barabino, Changes in phenotype and differentiation potential of human mesenchymal stem cells aging in vitro, *Stem Cell Res. Ther.* 9 (1) (2018) 131.
- [34] E. Gazi, J. Dwyer, N.P. Lockyer, J. Miyan, P. Gardner, C. Hart, M. Brown, N.W. Clarke, Fixation protocols for subcellular imaging by synchrotron-based Fourier transform infrared microspectroscopy, *Biopolymers Original Res. Biomol.* 77 (1) (2005) 18–30.
- [35] A.C.S. Talari, Z. Movasaghi, S. Rehman, I.U. Rehman, Raman spectroscopy of biological tissues, *Appl. Spectrosc. Rev.* 50 (1) (2015) 46–111.



Contents lists available at ScienceDirect

Spectrochimica Acta Part A: Molecular and Biomolecular Spectroscopy

journal homepage: www.elsevier.com/locate/saa

Intermolecular and low-frequency intramolecular Raman scattering study of racemic ibuprofen



J.J. Lazarević^{a,*}, S. Uskoković-Marković^b, M. Jelikić-Stankov^b, M. Radonjić^c, D. Tanasković^c, N. Lazarević^d, Z.V. Popović^d

^a Innovation center, Faculty of Technology and Metallurgy, University of Belgrade, Serbia

^b Faculty of Pharmacy, University of Belgrade, Serbia

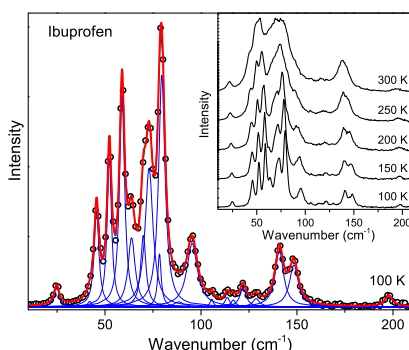
^c Scientific Computing Laboratory, Institute of Physics Belgrade, University of Belgrade, Pregrevice 118, 11080 Belgrade, Serbia

^d Center for Solid State Physics and New Materials, Institute of Physics Belgrade, University of Belgrade, Pregrevice 118, 11080 Belgrade, Serbia

HIGHLIGHTS

- Racemic ibuprofen Raman scattering spectra was measured at room and low temperatures.
- First principle calculations of the ibuprofen molecule dynamics properties were performed.
- Correlations between the molecule and crystal vibrations were established.

GRAPHICAL ABSTRACT



ARTICLE INFO

Article history:

Received 22 July 2013

Received in revised form 22 January 2014

Accepted 28 January 2014

Available online 12 February 2014

Keywords:

Spectroscopy
Raman
Ibuprofen
Low-temperature
Numerical calculations

ABSTRACT

We report the low-temperature Raman scattering study of racemic ibuprofen. Detailed analysis of the racemic ibuprofen crystal symmetry, related to the vibrational properties of the system, has been presented. The first principle calculations of a single ibuprofen molecule dynamical properties are compared with experimental data. Nineteen, out of 26 modes expected for the spectral region below 200 cm^{-1} , have been observed.

© 2014 Elsevier B.V. All rights reserved.

Introduction

Organic molecular crystals are characterized by a pronounced contrast between the strong covalent intramolecular interactions and the weak van der Waals intermolecular attractions or the

hydrogen bonding association. Whereas the intermolecular interactions are responsible for specific physical properties of the molecular compounds, the strong covalent bonds maintain the internal molecular structure. The vibrations within the molecular crystals can be of two types: internal vibrations (within the molecule) and external vibrations (between the molecules). Raman spectroscopy allows us to analyze these different kinds of motions. Consequently, external vibrations are closely related to the specific

* Corresponding author.

E-mail address: jasminalazarevic@hotmail.com (J.J. Lazarević).

physical properties of the molecular compounds, providing information on the stability of the physical state at molecular levels, and the nature of solid state transformations. Raman spectroscopy provides direct information on the phase transition from *in situ* investigations on molecular compounds exposed to a wide variety of environmental stress, since no special sample preparation is required. Thereby, Raman spectroscopy has important applications in the field of pharmaceutical sciences.

Ibuprofen (IBP), 2-(4-isobutylphenyl)propanoic acid, is a widely used non-steroidal anti-inflammatory drug having analgesic and antipyretic activities. It can be found in two enantiomeric forms: S(+)-IBP and R(-)-IBP, where the S-IBP is the pharmacologically active form. In fact, the commercial drug is the racemic mixture of these two forms and it appears at ambient temperature as a white crystalline powder. The ibuprofen racemic mixture in its crystalline phase I ((RS)-IBP) is stable up to the melting point $T_{mi} = 349$ K [1]. Recently, the existence of the second solid state phase of the racemic ibuprofen has been reported [2,3].

Although the information about the low-energy external vibrations is crucial for the identification of different solid state phases, previous Raman scattering and theoretical studies on (RS)-IBP vibration properties have been focused mainly on the internal (molecular) vibrations at energies larger than 200 cm^{-1} [4–7]. To the best of our knowledge, the low energy region of the (RS)-IBP Raman spectra has been reported only by Hédoux et al. [3]. The authors reported only three peak structures at about 20 cm^{-1} , 50 cm^{-1} and 80 cm^{-1} and assigned them as the phonon modes, whereas symmetry properties of the (RS)-IBP crystal structure suggest a large number of the external vibrations. No detailed analysis of the spectra in terms of the specific symmetry properties of (RS)-IBP has been performed. In this paper, detailed study of the low energy region of the (RS)-IBP Raman scattering spectra at various temperatures is presented. Vibrational properties of the (RS)-IBP is discussed in terms of the peculiarities of the (RS)-IBP crystal structure. Temperature dependent spectra are analysed by means of the anharmonicity model.

Experiment

Raman scattering measurements were performed using the Jobin Yvon T64000 Raman systems in backscattering micro-Raman configuration with 1800/1800/1800 grooves/mm gratings in subtractive regime. The external and second intermediate slits were set to $100\text{ }\mu\text{m}$, whereas lateral slits were adjusted so the minimum noise is achieved. The 514.5 nm line of a mixed Ar^+/Kr^+ gas laser was used as an excitation source. The corresponding excitation power density was less than 0.3 kW/cm^2 . Temperature dependent measurements were performed using LINKAM THMS 600 heating/cooling stage. All the Raman scattering spectra are corrected by the corresponding Bose factor $n(T)$.

Results and discussion

The structure of a single IBP molecule is presented in Fig. 1. Due to the low symmetry, all 93 A modes representing the vibrations of a single IBP molecule, are both infrared and Raman active. Commercially, IBP is found as a racemate in the form of the molecular crystals. (RS)-IBP crystallizes in the monoclinic type of structure with four ($Z = 4$) molecular units per unit cell [8–12]. The (RS)-IBP, R(-)- and S(+)-IBP enantiomers form a cyclic dimer across hydrogen bonds of their carboxylic groups through the center of inversion. This leads to an increase of a symmetry from the $P2_1$ for the S-IBP to $P2_1/c$ (C_{2h}^5) in the case of (RS)-IBP. The main implication of the inversion symmetry presence in the crystal is the separation of the Raman and infrared active modes.

In general, for the molecular crystals, two types of vibrations could be distinguished: external vibrations (vibrations between the molecules) and internal vibrations (vibrations within the molecules). Depending on the type of the motion, external vibrations could be translations (representing the translational motions of the molecules) or librations (representing the rotational motions of the molecules).

In order to determine the vibrational structure of the (RS)-IBP, the correlation method was applied [13]. By correlating the translational and the rotational modes of a single molecule to the site symmetry and the crystal symmetry (see Fig. 2), the external vibrational mode distribution at the Brillouin zone center (Γ point) was obtained:

$$\Gamma_{\text{Raman}} = 6A_g + 6B_g,$$

$$\Gamma_{\text{infrared}} = 5A_u + 4B_u,$$

$$\Gamma_{\text{acoustic}} = A_u + 2B_u$$

Thus one can expect 12 external modes to be observed in the Raman scattering experiment.

In the same manner, by establishing the correlation between the symmetry of the molecular vibrations, the site symmetry and the symmetry of the crystal through the peculiarities of the (RS)-IBP crystal structure (see Fig. 2), 186 internal modes ($93A_g + 93B_g$) are expected to be observed in the Raman scattering experiment. This substantial increase in the number of the observable vibrational modes for the molecular crystal in comparison to an isolated molecule is a consequence of the interactions between the molecules. Having in mind that the molecules are connected with very weak van der Waals interactions, the internal modes will usually appear as a $A_g - B_g$ doublets around the energies that correspond to the energies of the single molecule vibrations. Furthermore, the splitting within the doublets is rather small and thus they are typically observed as a single feature in the Raman scattering spectra.

Nature of the intermolecular bonds suggests that all external vibrations are expected to be found in the low energy part of the Raman spectra. However, ibuprofen is a highly flexible molecule, and thus one can also expect a number of low-lying internal doublets, each arising from a mode of the isolated molecule (see Fig. 2).

In order to determine the vibrational spectra of a single molecule, we perform first principle calculations of the IBP molecule dynamics properties, within density functional perturbation theory [14] as implemented in the QUANTUM ESPRESSO package [15]. We used scalar relativistic ultra-soft pseudopotentials, generated within general gradient approximations with Perdew–Burke–Ernzerhof exchange correlation functional. Structural parameters are relaxed so that total force acting on each atom is less than 10^{-4} Ry/a.u. In order to study the isolated molecule, the unit cell is made to be several times larger than the size of the molecule itself and all calculations are performed at the center of the Brillouin zone. Energy cut-offs for the wave functions and the electron densities are 60 Ry and 800 Ry respectively, determined to ensure a stable convergence. Calculated vibrational mode energies of a single S-IBP molecule in the low energy region are summarized in Table 1. Corresponding displacement patterns are presented in Fig. 1. We have also performed calculations on R-IBP and there are no significant changes in phonon energies between these two forms. Obtained energies of the vibrational modes at energies larger than 200 cm^{-1} are in good agreement with previously published data [4–7] and with our Raman (RS)-IBP measurements presented in Fig. 3(a).

According to the symmetry considerations for the (RS)-IBP crystal structure, 12 Raman active modes originating from the external vibrations are expected. From the single IBP molecule numerical calculations, we have found that in the spectral region under

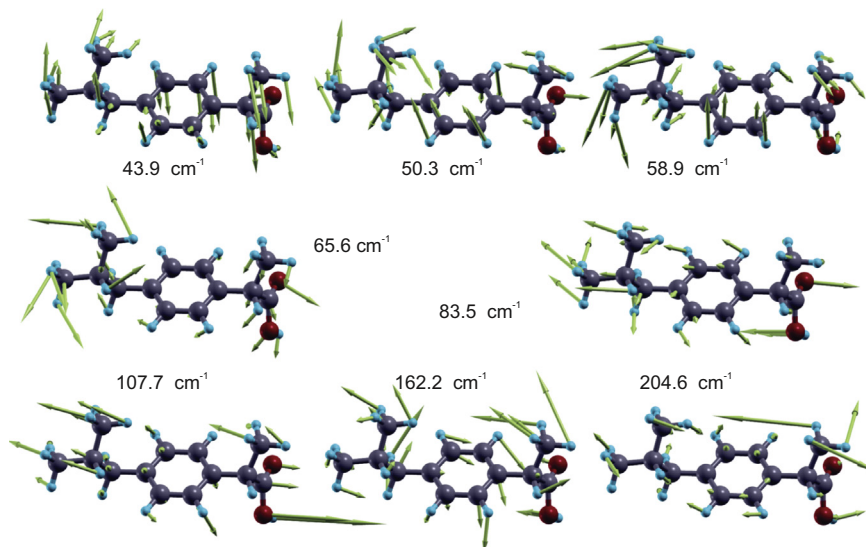


Fig. 1. Displacement patterns of the low energy Raman active vibrational modes of (RS)-IBP. The lengths of the arrows are proportional to the vibration amplitudes.

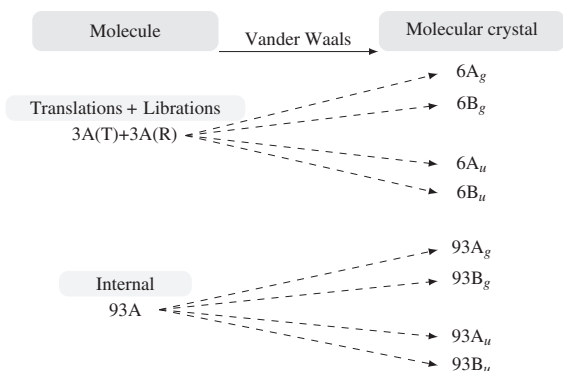


Fig. 2. Correlation diagram between the molecular and crystal vibrations.

Table 1

Calculated vibrational mode energies, symmetry and activity for a single S-IBP molecule in the low energy region.

Symmetry	Calculated energy (cm ⁻¹)	Activity
A	43.9	IR + R
A	50.3	IR + R
A	58.9	IR + R
A	65.6	IR + R
A	83.5	IR + R
A	107.7	IR + R
A	162.2	IR + R

200 cm⁻¹ 7 intramolecular doublets are expected, each arising from a mode of the isolated molecule. This give rise to the total of 26 Raman active modes to be observed in the spectral region under 200 cm⁻¹. The presence of both the internal and the external vibrational modes in the same spectral region indicates the strong mixing between the two types of vibrational modes [16–18].

Fig. 3(b) shows the low energy region Raman scattering spectra of (RS)-IBP measured at various temperatures. As one can see, at room temperature only four structures at about 21 cm⁻¹, 52 cm⁻¹, 74 cm⁻¹ and 138 cm⁻¹ can be clearly distinguished. This is in agreement with the findings of Hédoux et al. [3], where the authors observed three peaks at around 20 cm⁻¹, 50 cm⁻¹ and 80 cm⁻¹ and assigned them as phonon peaks. However, as already mentioned, symmetry of the system predicts a much larger

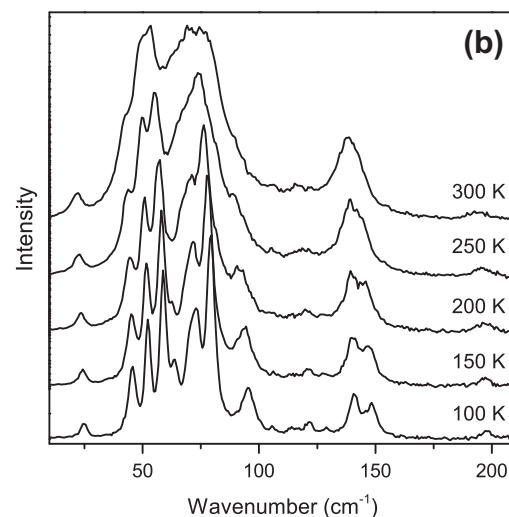
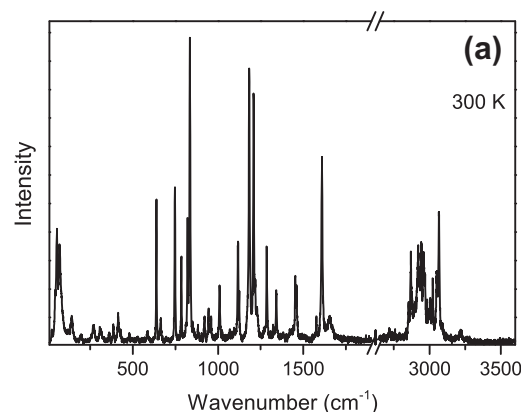


Fig. 3. (a) Wide range Raman scattering spectra of the (RS)-Ibuprofen. (b) The low energy region Raman scattering spectra of (RS)-Ibuprofen measured at various temperatures.

number of peaks and thus we should consider these structure to be multi-peak structures. In order to analyse these multi-peaks structure, we performed the low temperature measurements. In

general, with decreasing temperature linewidth of each mode decreases due to the anharmonicity effects [19]. Consequently, a large number of modes become observable at 100 K (see Fig. 3(b)).

Fig. 4 shows unpolarized Raman scattering spectra of (RS)-ibuprofen measured at 100 K. Solid lines represent deconvoluted spectra obtained by least-squares fitting with multiple Lorentzian line shapes. We were able to observe 19 out of 26 modes predicted by structural considerations. Energies of the observed modes are summarized in Fig. 4. Whereas all the modes below 140 cm^{-1} are expected to have mixed character to some extent, all additional modes above 140 cm^{-1} can be safely assigned as an intramolecular doublets.

Fig. 5(a) shows Raman scattering spectra of the peak structure around 145 cm^{-1} of (RS)-IBP measured at various temperatures. Although, only a single mode is predicted by the numerical calculation for the IBP molecule in this spectral region (see Table 1), two modes are clearly observed at low temperatures. Thus, this structure can be assigned as an $A_g - B_g$ doublet, as suggested by symmetry analysis (see Fig. 2). Energy separation within the doublet is related to the interaction between the molecules and the crystal structure of the sample. With increasing temperature the modes are shifted toward the lower wavenumbers and become progressively broader in accordance with anharmonicity effects (see Fig. 5(b)).

In general, temperature dependence of the vibrational mode energy, $\Omega(T)$ is usually governed by anharmonic effects. If, for the sake of simplicity, we assume a symmetric decay of the low lying optical vibration into two acoustic vibrations, the anharmonicity induced energy temperature dependence can be described with [19,20]:

$$\Omega(T) = \Omega_0 - C \left(1 + \frac{2}{e^x - 1} \right), \quad (1)$$

where Ω_0 is the Raman mode energy, C is the anharmonic constant and $x = \hbar\Omega_0/2k_B T$.

Fig. 5(c) shows the highest intensity low lying modes energy temperature dependence. Dashed lines represent calculated spectra by using Eq. (1). The best fit parameters are presented in Table 2. Good agreement between the experimental data and the calculated spectra suggest that the temperature dependence of the low energy (RS)-IBP Raman active modes is mainly driven by the anharmonicity effects. In general, knowledge about the Raman modes energy temperature dependence alone is not sufficient to separate the low lying internal from the external modes [21,22]. More complete approach for determination of the modes type

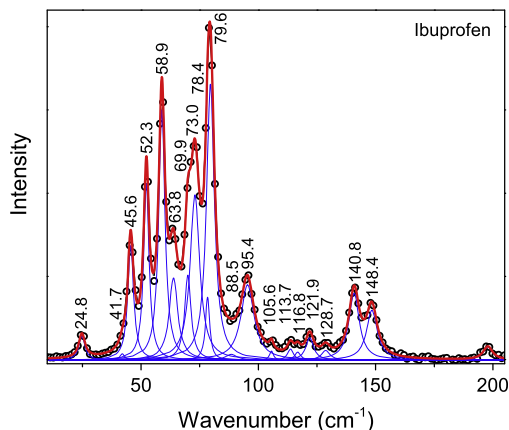


Fig. 4. Raman scattering spectra of (RS)-IBP measured at 100 K. Solid lines represent calculated spectra by using Lorentz profiles.

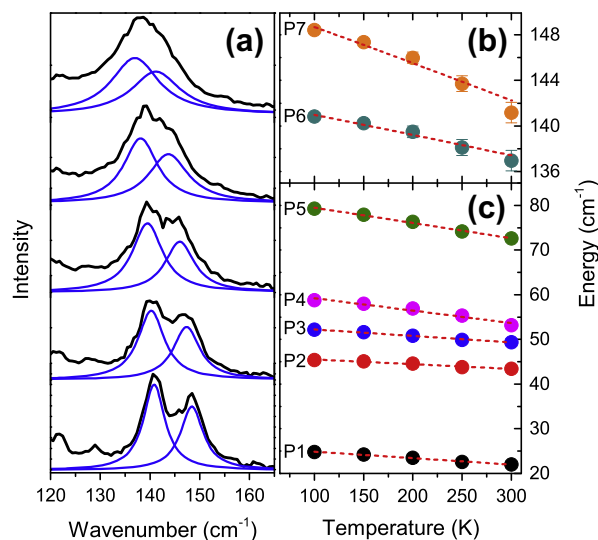


Fig. 5. (a) Raman scattering spectra of the double peak structure around 145 cm^{-1} of (RS)-IBP measured at various temperatures. (b and c) Energy temperature dependence of highest intensity Raman modes.

Table 2

Best-fitting parameters for Raman modes energy temperature dependence using Eq. (1).

	Ω (cm^{-1})	C (cm^{-1})		Ω (cm^{-1})	C (cm^{-1})
P1	26.3	0.13	P5	83.0	1.0
P2	46.6	0.18	P6	143.0	0.9
P3	53.7	0.28	P7	152.3	1.8
P4	62.0	0.6			

would require combination of pressure and temperature dependent measurements [22].

Conclusion

The Raman scattering spectra of the (RS)-IBP measured at various temperatures has been reported. Detailed analysis of the (RS)-IBP crystal symmetry, predicted 12 external modes for this system. According to the numerical calculations, appearance of internal vibrational modes is also expected in the low energy region of the spectra, mostly in terms of $A_g - B_g$ doublets, as in the case of the $141\text{--}148\text{ cm}^{-1}$ structure. Total of nineteen Raman active modes have been observed in the region below 200 cm^{-1} . Temperature dependence of the low energy (RS)-IBP Raman active modes is driven by anharmonicity effects.

Acknowledgments

This work was financially supported by the Serbian Ministry of Education, Science and Technological Development under the project III 46010. Part of this work was carried out at the Institute of Physics Belgrade supported by the Serbian Ministry of Education, Science and Technological development under Projects ON171032, III45018, ON171017. Numerical simulations were run on the AEGIS e-Infrastructure, supported in part by FP7 projects EGI-InSPIRE, PRACE-1IP and HP-SEE.

References

- [1] G.L. Perlovich, S.V. Kurkov, L.K. Hansen, A. Bauer-Brandl, Thermodynamics of sublimation, crystal lattice energies, and crystal structures of racemates and enantiomers: (+)- and (-)-ibuprofen, *J. Pharm. Sci.* 93 (2004) 654–666.

- [2] E. Dudognon, F. Dande, M. Descamps, N. Correia, Evidence for a new crystalline phase of racemic ibuprofen, *Pharm. Res.* 25 (2008) 2853–2858.
- [3] A. Hédoux, Y. Guinet, P. Derollez, E. Dudognon, N.T. Correia, Raman spectroscopy of racemic ibuprofen: evidence of molecular disorder in phase (II), *Int. J. Pharm.* 421 (2011) 45–52.
- [4] B. Rossi, P. Verrocchio, G. Viliani, I. Mancini, G. Guella, E. Rigo, G. Scarduelli, G. Mariotto, Vibrational properties of ibuprofencyclodextrin inclusion complexes investigated by Raman scattering and numerical simulation, *J. Raman Spectrosc.* 40 (2009) 453–458.
- [5] A. Jubert, M.L. Legarto, N.E. Massa, L.L. Tvez, N.B. Okulik, Vibrational and theoretical studies of non-steroidal anti-inflammatory drugs ibuprofen [2-(4-isobutylphenyl)propionic acid]; naproxen [6-methoxy-methyl-2-naphthalene acetic acid] and tolmetin acids [1-methyl-5-(4-methylbenzoyl)-1h-pyrrole-2-acetic acid], *J. Mol. Struct.* 783 (2006) 34–51.
- [6] M. Vueba, M. Pina, L. Batista de Carvalho, Conformational stability of ibuprofen: assessed by dft calculations and optical vibrational spectroscopy, *J. Pharm. Sci.* 97 (2008) 845–859.
- [7] L. Bondesson, K.V. Mikkelsen, Y. Luo, P. Garberg, H. gren, Hydrogen bonding effects on infrared and Raman spectra of drug molecules, *Spectrochim. Acta Part A: Mol. Biomol. Spectrosc.* 66 (2007) 213–224.
- [8] N. Shankland, C.C. Wilson, A.J. Florence, P.J. Cox, Refinement of ibuprofen at 100 K by single-crystal pulsed neutron diffraction, *Acta Crystallogr. Section C* 53 (1997) 951–954.
- [9] A.A. Freer, J.M. Bunyan, N. Shankland, D.B. Sheen, Structure of (S)-(+)-ibuprofen, *Acta Crystallogr. Section C* 49 (1993) 1378–1380.
- [10] L.K. Hansen, G.L. Perlovich, A. Bauer-Brandl, Redetermination and H-atom refinement of (S)-(+)-ibuprofen, *Acta Crystallogr. Section E* 59 (2003) o1357–o1358.
- [11] K. Shankland, W. David, T. Csoka, L. McBride, Structure solution of ibuprofen from powder diffraction data by the application of a genetic algorithm combined with prior conformational analysis, *Int. J. Pharm.* 165 (1998) 117–126.
- [12] N. Shankland, A.J. Florence, P.J. Cox, C.C. Wilson, K. Shankland, Conformational analysis of ibuprofen by crystallographic database searching and potential energy calculation, *Int. J. Pharm.* 165 (1998) 107–116.
- [13] W.G. Fateley, Infrared and Raman selection rules for molecular and lattice vibrations: the correlation method, Wiley Interscience, New York, 1972.
- [14] S. Baroni, S. de Gironcoli, A. Dal Corso, P. Giannozzi, Phonons and related crystal properties from density-functional perturbation theory, *Rev. Mod. Phys.* 73 (2001) 515–562.
- [15] P. Giannozzi, S. Baroni, N. Bonini, M. Calandra, R. Car, C. Cavazzoni, D. Ceresoli, G.L. Chiarotti, M. Cococcioni, I. Dabo, A.D. Corso, S. de Gironcoli, S. Fabris, G. Fratesi, R. Gebauer, U. Gerstmann, C. Gougoussis, A. Kokalj, M. Lazzeri, L. Martin-Samos, N. Marzari, F. Mauri, R. Mazzarello, S. Paolini, A. Pasquarello, L. Paulatto, C. Sbraccia, S. Scandolo, G. Sclauzero, A.P. Seitsonen, A. Smogunov, P. Umari, R.M. Wentzcovitch, Quantum espresso: a modular and open-source software project for quantum simulations of materials, *J. Phys.: Condens. Matter* 21 (2009) 395502.
- [16] G. Filippini, C.M. Gramaccioli, Lattice-dynamical calculations for tetracene and pentacene, *Chem. Phys. Lett.* 104 (1984) 50–53.
- [17] R.G. Della Valle, E. Venuti, L. Farina, A. Brillante, M. Masino, A. Girlando, Intramolecular and low-frequency intermolecular vibrations of pentacene polymorphs as a function of temperature, *J. Phys. Chem. B* 108 (2004) 1822–1826.
- [18] N. Lazarevic, M.M. Radonjic, D. Tanaskovic, R. Hu, C. Petrovic, Z.V. Popovic, Lattice dynamics of fcsb 2, *J. Phys.: Condens. Matter* 24 (2012) 255402.
- [19] M. Balkanski, R.F. Wallis, E. Haro, Anharmonic effects in light scattering due to optical phonons in silicon, *Phys. Rev. B* 28 (1983) 1928–1934.
- [20] N. Lazarević, Z.V. Popović, R. Hu, C. Petrovic, Evidence for electron–phonon interaction in $Fe_{1-x}M_xSb_2$ ($M = Co$ and Cr ; $0 \leq x \leq 0.5$) single crystals, *Phys. Rev. B* 81 (2010) 144302.
- [21] P.N. Prasad, R. Kopelman, External, internal and semi-internal vibrations in molecular solids: spectroscopic criteria for identification, *Chem. Phys. Lett.* 21 (1973) 505–510.
- [22] R. Zallen, M.L. Slade, Influence of pressure and temperature on phonons in molecular chalcogenides: crystalline As_4S_4 and S_4N_4 , *Phys. Rev. B* 18 (1978) 5775–5798.



Contents lists available at ScienceDirect

Spectrochimica Acta Part A: Molecular and Biomolecular Spectroscopy

journal homepage: www.elsevier.com/locate/saa

Probing primary mesenchymal stem cells differentiation status by micro-Raman spectroscopy

J.J. Lazarević^a, T. Kukolj^b, D. Bugarski^b, N. Lazarević^{a,*}, B. Bugarski^c, Z.V. Popović^{a,d}^aCenter for Solid State Physics and New Materials, Institute of Physics Belgrade, University of Belgrade, Pregrevica 118, Belgrade 11080, Serbia^bLaboratory for Experimental Hematology and Stem Cells, Institute for Medical Research, University of Belgrade, Belgrade 11000, Serbia^cDepartment of Chemical Engineering, Faculty of Technology and Metallurgy, University of Belgrade, Karnegijeva 4, Belgrade 11060, Serbia^dSerbian Academy of Sciences and Arts, Knez Mihailova 35, Belgrade 11000, Serbia

ARTICLE INFO

Article history:

Received 17 September 2018

Accepted 21 January 2019

Available online 29 January 2019

Keywords:

Raman spectroscopy

Stem cells

Differentiation

ABSTRACT

We have employed micro-Raman spectroscopy to get insight into intrinsic biomolecular profile of individual mesenchymal stem cell isolated from periodontal ligament. Furthermore, these cells were stimulated towards adipogenic, chondrogenic, and osteogenic lineages and their status of differentiation was assessed using micro-Raman spectroscopy. In both cases, glass coverslips were used as substrates, due to their wide availability and cost effectiveness. In all sample groups, the same type of behavior was observed, manifested as changes in Raman spectra: the increase of relative intensity of protein/lipid bands and decrease of nucleic acid bands. Comprehensive statistical analysis in the form of principal component analysis was performed, which revealed noticeable grouping of cells with the similar features. Despite the inhomogeneity of primary stem cells and their differentiated lineages, we demonstrated that micro-Raman spectroscopy is sufficient for distinguishing cells' status, which can be valuable for medical and clinical application.

© 2019 Published by Elsevier B.V.

1. Introduction

In the era of regenerative medicine development, stem cells are in the center of attention, bringing hope for treating conditions and diseases presently incurable. In general, these expectations arise from unique qualities of these cells, which include self-renewal and multilineage differentiation potential *in vitro*. When it comes to potential clinical application of stem cells, from the aspect of differentiation capacity, embryonic stem cells (ESCs) and induced pluripotent stem cells (iPSCs) provide the greatest possibilities. However, it is well documented that both ESCs and iPSCs can form teratoma which directly restricts their therapeutic application. On the other hand, considering relatively simple isolation procedures, without ethical issues that follow manipulation of ESCs, mesenchymal stem cells (MSCs) have advantage over ESCs and iPSCs. Therefore, MSCs are promising agents in cell therapy and tissue engineering [1,2]. More than forty years ago, MSCs were discovered in bone marrow, but today it is known that this heterogenous population of cells resides in tissues and organs throughout the adult organism, where their primary role

is maintenance of tissue regeneration and tissue homeostasis [3,4]. According to The International Society for Cellular Therapy, minimal criteria for characterisation of human MSCs are plastic adhesion with expression of CD73, CD90, and CD105 surface markers and lack of hematopoietic markers CD34-, CD45-, CD14-, CD79α-, HLA-DR-, and multilineage differentiation potential into osteoblasts, adipocytes, and chondroblasts [5]. Even though MSCs possess common cellular features, it is generally accepted that, due to tissue origin, donor age, culture conditions, these cells exhibit variable regenerative capacity [6,7]. Along with differentiation potential, an important part in considering MSCs as possible new therapeutic agents is their ability of immune response modulation (directly, through cell-to-cell contact or indirectly, by secretion of soluble factors) [8]. Originally, it was reported that MSCs can alter immune response in hypoimmunogenic manner, but their role in immunity is still the subject of extensive research [9].

Within regenerative dentistry, there is a great interest in development of novel therapeutic strategies related to the recovery of periodontium. As tooth supportive tissue, periodontium is directly responsible for appropriate incorporation of synthetic implants which today represents one of the main methods of medical treatment for curing dental defects. However, damaged periodontal tissue has limited capacity for regeneration and is often influenced by inflammation that can severely hamper periodontal structure,

* Corresponding author.

E-mail address: nenadl@ipb.ac.rs.

disabling implantation and tooth restoration. Periodontal ligament is a soft connective tissue which anchors tooth to the alveolar bone. Hence, the exploration of human periodontal ligament stem cells (hPDLSCs), as potential cell source for reconstructive dentistry, strongly contributes to the improvement of periodontal therapies [10–12]. Previously is demonstrated that PDLSCs fulfill criteria for MSCs identification and characterisation [13,14], set by International Society for Cellular Therapy [5,15]. Keeping in mind that the origin tissue of PDLSCs is periodontal ligament and that the main role of cells within this tissue is maintenance of mineralization level [16,17], it is expected for PDLSCs to be more osteogenic than adipogenic committed when compared to MSCs derived from other sources [18,19].

Regarding heterogeneity of MSCs, carefully performed characterisation of these cells and thoroughly monitored process of their differentiation, before further manipulation, is of great significance for their usage [20]. Various techniques are available in this field, such as immunocytochemistry, flow cytometry, mass spectrometry or gene expression analyses. However, these methods mostly imply disruption of cell integrity and, at the same time, they can be time consuming and require expensive biomarkers for each cell type [21]. Destructiveness comes out as the dominant drawback of these techniques. This gives rise to a need for non-invasive, non-destructive and fast technique, which would be able to monitor stem cells behavior, including differentiation process [20,21]. Owing to its features, Raman spectroscopy appears to be a promising candidate. Regarding clinical applicability, no sample preparation or a minimal preparation, is important feature of Raman spectroscopy. It is also suitable for measurements in aqueous solutions. The outcome of Raman scattering measurement is a vibrational spectrum in which macromolecules, such as proteins, nucleic acids, carbohydrates, and lipids, are presented with the most pronounced vibration modes of different chemical bonds. Interactions of molecules are also visible. Accordingly, Raman spectrum is a fingerprint of the analysed sample. In past decade, the interest in performing this type of analysis on stem cells is well documented [21–30].

Currently, advanced Raman setups are used in biomedical researches [31]. Most of the studies in the field of stem cells biology were performed with more experimentally demanding Raman spectroscopy experiments, such as Coherent anti-Stokes Raman spectroscopy (CARS), Raman tweezers, Tip enhanced Raman spectroscopy (TERS), or Surface enhanced Raman spectroscopy (SARS), due to their higher sensitivity. As far as we know, great number of these studies were focused on live murine and human ESCs [22–26], and spectral mapping of live and apoptotic ESCs [27], but the interest in mesenchymal stem cells is also noticeable [28,29,21]. One of the Raman studies on MSCs was performed to characterise the Raman spectra of bone marrow-derived MSCs and to study the effect of different inducers on their differentiation towards osteogenic lineage [30]. Further, Raman spectroscopy was assessed as the analytical tool which could be used for characterisation and identification of rhesus monkey mesenchymal stem cells from different age groups (fetal to juvenile) [32]. Moreover, Raman spectroscopy was used to map the distribution of different biomolecules within two types of stem cells: adult human bone marrow-derived MSCs and human ESCs, and to identify Raman spectral characteristics which distinguish genetically abnormal and transformed stem cell from normal ones [33]. Another study was dedicated to viability transitions detection of umbilical cord mesenchymal stem cells (hUC-MSCs) by micro-Raman spectroscopy, where the authors proposed that the viability of hUC-MSCs can be described with three peaks of certain energies [28].

Although numerous Raman studies of different stem cell lineages have been performed [22–26], it is still unclear whether Raman spectroscopy can unambiguously distinguish differentiation status of primary stem cells such as hPDLSCs. In order to

address this matter, Raman scattering study of undifferentiated and differentiated hPDLSCs (osteogenic, chondrogenic, and adipogenic cells) has been performed. To assure multilineage mesenchymal differentiation capacity of hPDLSCs, standard biological detection of adipogenesis, chondrogenesis, and osteogenesis was conducted.

In general, the widespread applicability of this technique demands simplicity of the experimental setup and the availability of used substrates. In medicine, the most commonly used substrates are made of glass, which may be challenging for Raman spectroscopy, due to contributions to the sample spectrum. Besides limiting the spectral region that can be probed in the light scattering experiment it also hinders signal to noise ratio. The aim of this work was to determine the analytical ability of micro-Raman spectroscopy in commonly available experimental configuration, in order to assess differentiation status of hPDLSCs, with minimal sample processing, on glass substrates. Direct comparison of the primary hPDLSCs and differentiated hPDLSCs Raman spectra, as well as statistical analysis, revealed clear distinction between these groups. This approach could vastly simplify diagnostics and promote clinical application of MSCs.

2. Experiment

2.1. Isolation and Cultivation of Human Periodontal Ligament Stem Cells

Human PDLSCs were isolated from normal impacted third molars, as described elsewhere [14]. In brief, following the informed consent, tissues were collected from healthy patients aging 18–25 years, subjected to the procedure of tooth extraction for orthodontic reasons, at the Department of Oral Surgery of the Faculty of Dental Medicine, the University of Belgrade. All treatments were performed according to the approved ethical guidelines set by Ethics Committee of the Faculty of Dental Medicine, the University of Belgrade and Declaration of Helsinki. Directly after tooth extraction, periodontal tissues were carefully detached from the mid-third of the root surface, minced into small pieces and placed in a 25 cm² flask with Dulbecco's modified Eagle's medium (DMEM; PAA Laboratories, Pasching, Austria) supplemented with 10% fetal bovine serum (FBS; PAA Laboratories), 100 U/ml penicillin and 100 µg/ml streptomycin (PAA Laboratories), and cultured at 37 °C in a humidified atmosphere containing 5% CO₂, with medium exchange every third day. When the 80% to 90% confluence was reached, the cells were passaged regularly in growth medium (GM-DMEM with 10% FBS) using 0.05% trypsin with 1 mM EDTA (PAA Laboratories) and for this study cells from third to sixth passages were used. Further on, considering the minimal criteria for characterisation of MSC [5] immunophenotype of hPDLSCs and their multipotent differentiation capacity towards osteogenic, chondrogenic, and adipogenic lineages were confirmed as previously reported [14].

2.2. Sample Preparation

For Raman measurements, hPDLSCs were seeded on rounded glass coverslips in 24-well plate (2 × 10⁴ cells per well) and grown in standard cultivation conditions. Simultaneously, cells were seeded in 24-well plate (2 × 10⁴ cells per well) to follow differentiation by regular *in vitro* staining. When the confluence was reached, cells were induced to differentiate into osteogenic, chondrogenic and adipogenic lineages by specific differentiation medium. Osteogenic differentiation medium contained DMEM supplemented with 5% FBS, 100 U/ml penicillin/streptomycin, 50 µM ascorbic acid-2-phosphate and 10 mM β-glycerophosphate (both from Sigma-Aldrich). Chondrogenic medium contained DMEM with 5% FBS, 2 ng/ml of transforming growth

factor- β 1 (TGF- β ; R&D Systems, Minneapolis, MN, USA), 50 μ M ascorbic acid-2-phosphate, 10 nM dexamethasone, 100 U/ml penicillin/streptomycin. Adipogenic medium contained 5% FBS in DMEM, 100 U/ml penicillin/streptomycin, 100 μ g/ml isobutyl-methyl xanthine (IBMX; Sigma-Aldrich), 1 μ M dexamethasone and 10 μ g/ml insulin (Sigma-Aldrich). With regular medium exchange, osteogenesis and chondrogenesis were evaluated after three weeks of cultivation, whereas adipogenesis was induced during four weeks. As for the control samples, cells were cultivated in GM with 5% FBS during the corresponding time. After this period, hPDLSCs were washed with saline buffer, fixed with methanol for 10 min at room temperature and washed with distilled water just before Raman spectroscopy was performed. Standard *in vitro* examination of differentiation process was performed after cells had been fixed and stained with specific dye. Intracellular lipid droplets were observed by Oil Red O (Merck Chemicals, Darmstadt, Germany) staining, while Safranin O confirmed cartilage-specific proteoglycan formation. Alizarin red was used to visualize calcium deposition and mineralization of extracellular matrix (see Fig. 1). Optical microscope with digital camera was used for cell morphology analysis and imaging.

2.3. μ -Raman Spectroscopy

Raman scattering measurements were performed using TriVista 557 Raman system in backscattering μ -Raman configuration. As an excitation source, 532 nm laser line of the Coherent VerdiG laser was used. The focusing on the sample was achieved by using $\times 100$ microscope objective, $NA = 0.80$. The laser spot diameter in our experimental configuration was $\approx 4 \mu$ m. In order to avoid any possible sample damage and/or temperature related effect, the laser power at the sample plain was kept at low levels, ≈ 1 mW. Acquisition time was 900 s. More details on Raman scattering experiment can be found in the Section S1 of the Supplementary Information.

From the aspects of vibrational spectroscopy, which can independently probe a single vibration within a molecule or a crystal, biological samples consisting of various types of macro-molecules, represent rather complicated systems. In these systems, only vibrational bands, consisting of numerous vibrations of the same type, can be taken into consideration, rather than a single vibration. Consequently, the changes of biological system (e.g. single cell) composition, may result in a change of certain Raman bands intensities.

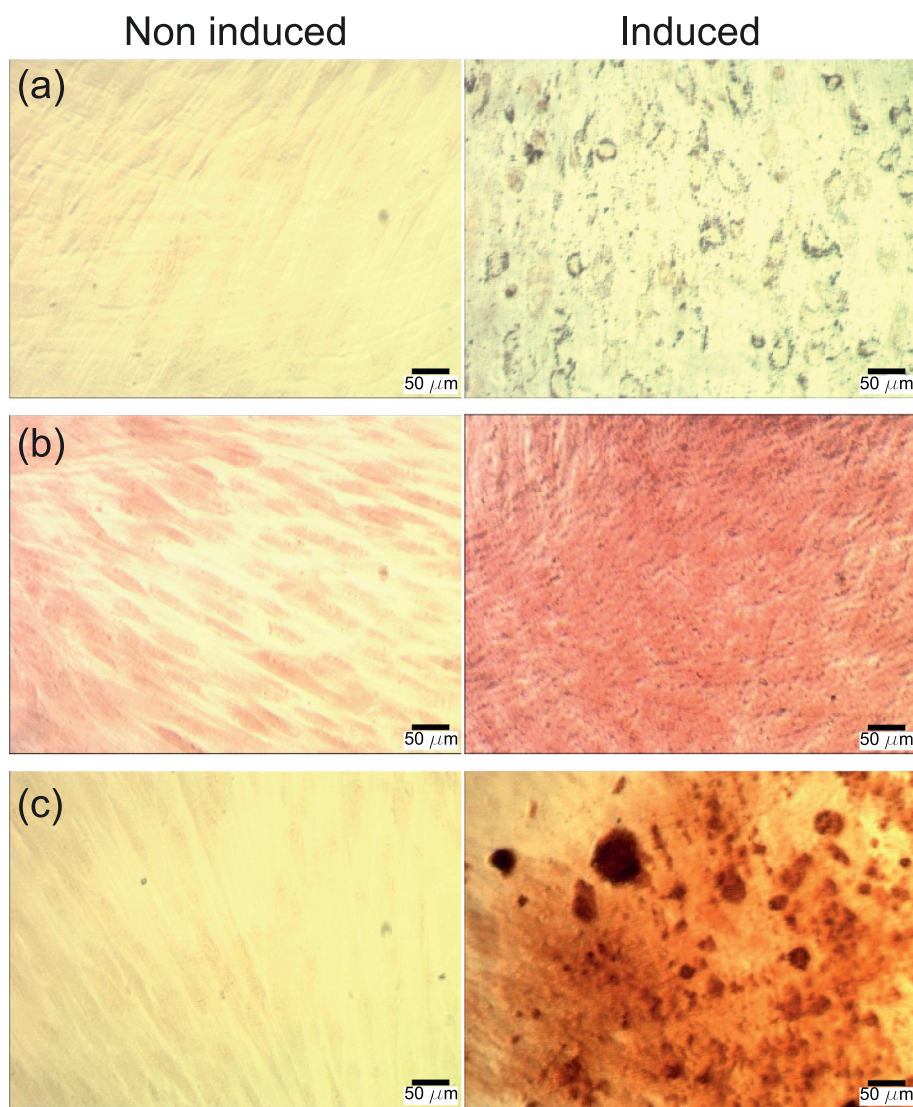


Fig. 1. Multilineage differentiation potential of hPDLSCs. (a) Oil Red O staining showed presence of intracytoplasmic lipid droplets confirming adipogenic differentiation. (b) Chondrogenic differentiation was demonstrated by positive staining of proteoglycans with Safranin O. (c) Positive Alizarin red staining of extracellular matrix mineralization confirmed osteogenic differentiation.

It should be taken into account that when probing a single cell, due to its complex inner structure, there might be small variations in Raman spectra for the data collected at different positions. To obtain single spectra representative for each of the cells, recorded spectra were averaged. The preliminary experiment involved investigation of 54 cells of Batch 1. For every cell lineage, 9 hPDLSCs and 9 differentiated cells were analysed by probing each cell at 10 randomly chosen positions. The results of the analysis performed on the full set of data as well as on the sub-set including three random positions, revealed no qualitative difference. This implies that for our experimental configuration and for the samples under investigation, three randomly chosen positions are sufficient to make qualitative conclusions. Having in mind statistical treatment of the results, a total of 1080 spectra from 360 cells were recorded and analysed in the main experiment.

2.4. Data Processing and Analysis

Prior to the analysis, all Raman spectra were processed by subtracting the contributions from substrate (see Fig. 2 (a)), as well as biological fluorescence. No spectral smoothing of the samples spectra has been performed. On the other hand, the substrate spectrum was obtained separately with greater acquisition time and statistics and post-processed by Savitzky–Golay filter. Right inset on Fig. 2 (a) compares the substrate and the mean of 540 hPDLSCs Raman spectra. Significantly smaller noise level of the (glass) substrate spectrum indicates absence of its contribution to hPDLSCs spectra statistics. Due to the substantial increase of the substrate spectral weight at lower energies, our analysis was limited to the region above 1000 cm^{-1} .

The absolute value of Raman intensity is not usually a reliable quantity. Even small variations in the experimental conditions may

produce the “artificial” variations of Raman intensity. In order to exclude this possible uncertainty, all spectra were normalised onto the peak at about 1660 cm^{-1} , which is present with high intensity in all obtained spectra.

Besides the direct comparison of spectra obtained from stem cells and differentiated cells, a multivariate statistical method, principal component analysis (PCA), was employed [40,20,25,22]. The main goal of PCA is to reduce the effective dimensionality of the experimental data set by determining the orthonormal basis of loading vectors in a way that the greatest variance is projected onto the first coordinate, the second greatest variance is projected onto the second coordinate, and so on. The outcome of this analysis is clear grouping of Raman spectra according to their mutual features. Prior to performing PCA, the spectral data were subtracted by the mean spectrum and divided by its standard deviation [40,22].

3. Results and Discussion

To get insight on how hPDLSCs differentiation status reflects on Raman spectra, three sets of Raman experiments were performed. The samples were set in two batches. For every lineage, spectra were obtained for 30 hPDLSCs and 30 differentiated cells (hPDLSC grown in standard cultivation medium for the corresponding time for each differentiation). The spectrum of every cell was measured three times on each of three randomly chosen positions within the cell in order to incorporate possible variations within a single cell and test the approach sufficiency for observing the difference between cell lineages.

Fig. 2 (b) shows Raman spectrum of hPDLSCs obtained by averaging spectra of all control samples. The main contribution to the hPDLSCs Raman spectrum for the region under consideration comes from nucleic acids, proteins and lipids [24,28,41,23,37–39]. Spectral features of nucleic acids originate from the individual purine and pyrimidine bases (adenine, thymine, guanine, cytosine, and uracil), as well as from backbone structure of DNA and RNA, whereas protein spectral features include contributions from aromatic amino acids (phenylalanine, tryptophan, and tyrosine), amide groups of secondary protein structures (α -helices, β -sheets, and random coils), and various vibrations of carbon atoms bonded with nitrogen and/or other carbon atoms [38]. Different vibrations within the hydrocarbon chain (e.g. C–C stretching, CH_2 and CH_3 scissoring and twisting) present specific features of lipids in Raman spectra [35]. Principally, various contributions may overlap, making the determination of the potential changes in Raman spectra of undifferentiated and differentiated hPDLSCs a formidable task. As can be seen from Fig. 2 (b), numerous vibrational bands have been observed in hPDLSCs Raman spectrum. The most pronounced bands are assigned according to the literature [24,28,41,23, 34–39] and summarized in Table 1.

Fig. 3 (a)–(c) shows averaged hPDLSCs Raman spectra of control samples, differentiated cells (adipocytes, chondroblasts, and osteoblasts, respectively) of both batches, as well as corresponding pairs' differences. Although the overall spectral features in these pairs of spectra look almost the same, after the subtraction, the difference is more pronounced. General conclusion, consistent with the literature data [22,25], is that relative intensities (with regard to 1660 cm^{-1} peak structure intensity) of nucleic acids and proteins, are able to distinguish stem cells from more mature cells. In the case of adipogenic differentiation, a slight decrease of the relative intensity of the band at 1100 cm^{-1} and increase of the relative intensity of peaks at about 1353 cm^{-1} , 1447 cm^{-1} , and 1590 cm^{-1} (see Fig. 3 (a)) is observed. According to Table 1, this might be understood as slight reduction of nucleic acids and enhancement of proteins and lipids. On the other hand, the possible increase of the band at 1735 cm^{-1} , assigned to lipids (esters), is absent. Explanation for this lies in the fact that these cells do not originate from

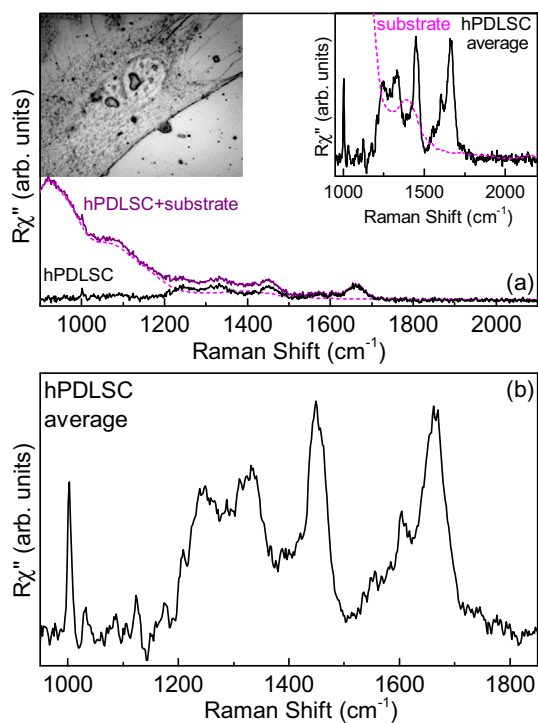


Fig. 2. (a) Raman scattering spectra of hPDLSCs on glass, glass substrate and their difference. Left inset: Image of hPDLSCs. Right inset: Comparison between the substrate and the mean of 540 hPDLSCs Raman spectra. (b) The mean of 540 hPDLSCs Raman spectra.

Table 1

Vibrations in hPDLSCs and their energies noticed in Raman spectrum. (A) adenine, (U) uracil, (C) cytosine, (T) thymine, (G) guanine, (Phe) phenylalanine, (Trp) tryptophan, (Tyr) tyrosine, (vib) vibration, (bg) bending, (br) breathing, (bk) backbone, (def) deformation, (tw) twist, (sym) symmetric, (asym) asymmetric, and (str) stretch [28,23,34–39].

Energy (cm ⁻¹)	Assignment
1004	Phe
1032	Phe
1061	C—N and C—C str
1080	PO ₂ ⁻ sym str
1085	C—O str
1105	PO ₂ ⁻ str (sym)
1130	C—N and C—C asym str
1155	C—C and C—N str of proteins
1165	C—O str, COH bg
1172	G ring str
1178	CH ben Tyr
1209	C—C ₆ H ₅ str, Phe, Trp
1228	Asym phosphate str
1250	T, amide III _β
1260	N—H and C—H bg (amide III/distorted)
1265	Amide III _α
1315	G, CH def.
1332	DNA purine bases (CH ₃ CH ₂ wagging mode of polynucleotide chain)
1450	CH ₂ str def of methylene group in lipids
1456	CH def.
1556	Amide II
1604	Phe, Tyr
1654	Amide I, α helix
1670	Amide I, β sheet

adipose tissue [18,19]. When it comes to the case of chondrogenic differentiation, higher relative intensities of the peaks at 1065 cm⁻¹, 1250–1450 cm⁻¹, and 1630 cm⁻¹ are exhibited (Fig. 3 (b)). These

changes arise from higher content of proteins and proteoglycans [42,43]. Regarding the osteogenic differentiation, spectral changes between hPDLSCs and their differentiated pairs (Fig. 3 (c)) originate from the lower relative intensities of the bands in the region from 1170 cm⁻¹ to 1220 cm⁻¹ and from 1450 cm⁻¹ to 1490 cm⁻¹, and higher relative intensities at about 1045 cm⁻¹, 1070 cm⁻¹, and 1600 cm⁻¹. These changes are caused by decrease in amino acids and likely lipids, and increase in carbonates and phosphates, as expected. This decrease of the band intensity in the region that most likely correspond to lipids, might be understood as a change in proteins to lipids ratio. Typical spectral marker for this type of cells is hydroxyapatite, but due to spectral interference from the substrate (glass), it is out of spectral range of interest in this study [43]. Consistently observed spectral changes during the differentiation process (the increase of protein bands and decrease of nucleic acid bands in differentiated cells) are in accordance with the literature [22,25]. The possible explanation for this behavior is that, as cells differentiate, they gradually begin to use up the pool of mRNA to support the synthesis of new, cell lineage specific proteins [22].

Although the direct comparison between hPDLSCs and their differentiated lineages Raman spectra gave us means to distinguish cell differentiation status, it is demanding and require detailed analysis of the spectra. However, if we utilize the Raman spectra as characteristic fingerprints of the cells under investigation, PCA can be employed for pattern recognition and grouping. Fig. S1 of the Supplementary information summarizes loading vectors for the main PCs. It is noticeable that a certain loading vector or their linear combination fully describe corresponding difference spectra shown in Fig. 3 (a)–(c). Consequently, the same conclusions can be made as in previous paragraph. Fig. 3 (d)–(f) shows score plots calculated independently using PCA for three groups of control hPDLSCs samples and their differentiated lineages'

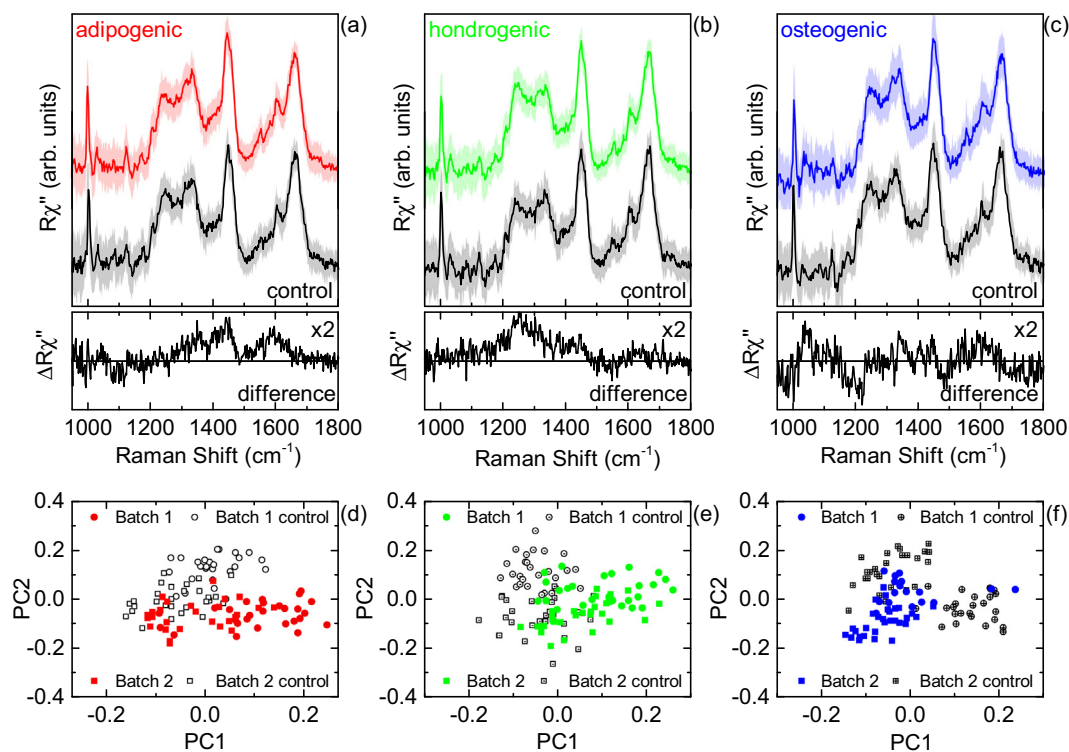


Fig. 3. (a)–(c) Averaged Raman spectra (black lines) of hPDLSCs (control samples), differentiated hPDLSCs (adipogenic, chondrogenic, and osteogenic lineages) and difference spectrum between these two groups of cells. Standard deviation for each lineage and control group is presented with the colored areas. (d)–(f) Score plots calculated independently using PCA for three groups of control hPDLSCs and differentiated hPDLSCs Raman spectra.

Raman spectra. In all three cases, two groups can be observed, with each grouping corresponding to a particular cell lineage. Furthermore, within each grouping, sub-groupings are noticed, indicating variations and inhomogeneity between the batches. In fact, this is not surprising since these are primary cells and the higher level of inhomogeneity is expected. In the following paragraphs, the attention will be focused on the analysis within the batches.

Fig. 4 summarizes adipogenic, chondrogenic, and osteogenic lineages score plots for Batches 1 and 2. Although the separation between data point groupings can be observed for both batches, it is more pronounced for Batch 1. Most likely, this is a consequence of higher inhomogeneity within the Batch 2.

In the next step, we wanted to test whether the same approach can be used to distinguish different types of differentiated cells (adipocytes, chondroblasts, and osteoblasts). For this purpose, the data from all three sets of experiments had been combined and PCA performed, for both batches. The obtained score plots are presented in Fig. 5. Shaded areas represent 1σ 2D confidence level. Remarkably, very good grouping of the different cell lineages has been observed for Batch 1. Less separation of different cell groups was observed for Batch 2, in agreement with the results presented in Fig. 4. Additionally, PCA indicates the variations within hPDLSCs (in particular for Batch 2) although this was not so obvious in direct comparison. When PCA was applied on hPDLSCs from all three control groups and compared with differentiated hPDLSCs data, it could be noticed that even though small variations are present, control hPDLSCs retain characteristics of stem cells, suggesting these cell populations are not homogeneous. Keeping that in mind, spectral analyses of hPDLSCs are in accordance with data obtained by traditional MSCs characterisation methods that also emphasize heterogeneity of MSCs population. As being primary cells, cellular diversity of MSCs is a result of isolation methods and culture conditions. Further, the absence of unique MSCs biomarkers makes these cells still highly difficult for molecular identification

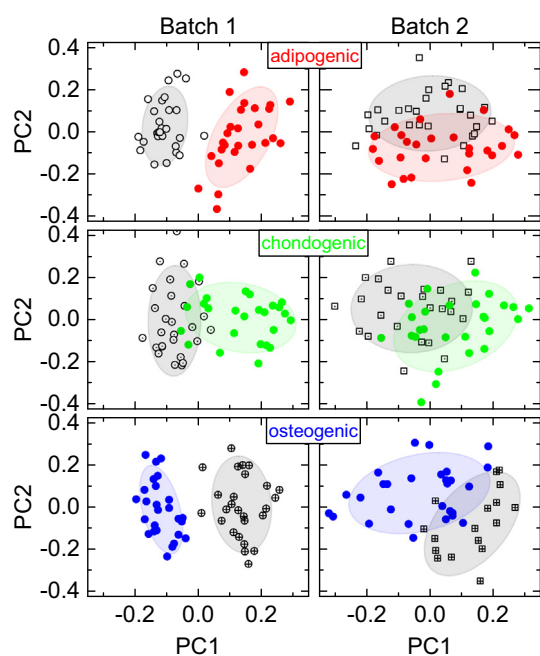


Fig. 4. Score plots calculated independently using PCA for three groups of control (black) and differentiated (adipogenic, chondrogenic, and osteogenic lineages) hPDLSCs samples Raman spectra in two batches. Shaded areas represent 1σ 2D confidence level.

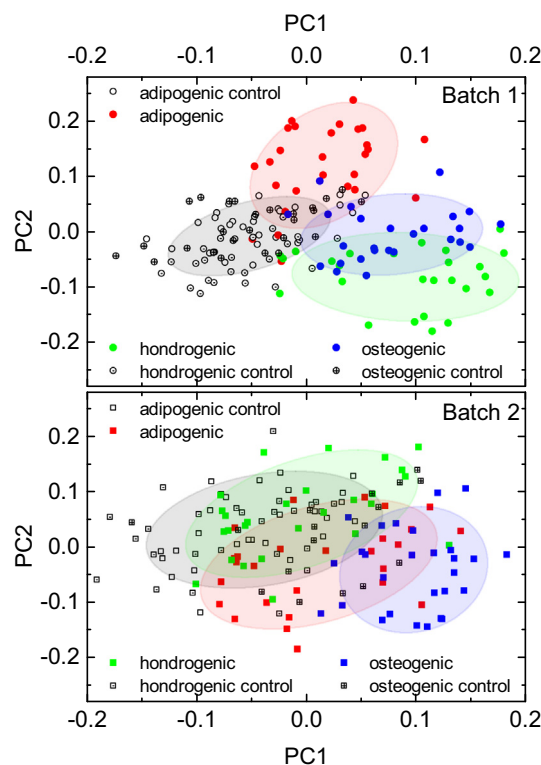


Fig. 5. PCA performed on all obtained Raman spectra of four groups of cells including nondifferentiated hPDLSCs (control) and differentiated hPDLSCs (osteogenic, chondrogenic and adipogenic lineages) for different batches. Shaded areas represent 1σ 2D confidence level.

and characterisation [5,44]. Thus, our results suggest the possibility of the Raman spectroscopy application in characterisation of MSCs.

4. Conclusion

In this study, the applicability of micro-Raman spectroscopy for probing primary hPDLSCs differentiation status on glass substrate was demonstrated. In direct comparison of hPDLSCs and differentiated cells Raman spectra, the difference in the relative intensities of certain marker bands has been observed. Additionally, statistical analysis of fingerprint Raman spectra of the cells using PCA, revealed distinct groupings based on the similar features. This gives a possibility of devising the procedure not only for fast and simple detection of different mesenchymal stem cell lineages, but also for the variations within. Furthermore, due to minimal preparation requirements and independency on the reagents that are necessary in standard biological techniques, Raman spectroscopy can be used as an additional method in MSCs characterisation. From the standpoint of MSCs utilization in biomedicine, simplification of the procedures in cell identification could significantly facilitate research in the field of stem cell biology.

Acknowledgments

We gratefully acknowledge M. Milić and M. Andrić for supplying the periodontal ligament tissue and Dr. N. Paunović for constructive discussions on the subject. This work was supported by the Ministry of Education, Science, and Technological Development of the Republic of Serbia, Serbia under Projects No. III46010, III45018, and ON175062.

Appendix A. Supplementary data

Supplementary data to this article can be found online at <https://doi.org/10.1016/j.saa.2019.01.069>.

References

- [1] X. Wei, X. Yang, Z. p. Han, F. f. Qu, L. Shao, Y. f. Shi, Mesenchymal stem cells: a new trend for cell therapy, *Acta Pharmacol. Sin.* 34 (6) (2013) 747–754.
- [2] D. Howard, L.D. Buttery, K.M. Shakesheff, S.J. Roberts, Tissue engineering: strategies, stem cells and scaffolds, *J. Anat.* 213 (1) (2008) 66–72.
- [3] Y. Sato, H. Araki, J. Kato, K. Nakamura, Y. Kawano, M. Kobune, T. Sato, K. Miyanishi, T. Takayama, M. Takahashi, et al. Human mesenchymal stem cells xenografted directly to rat liver are differentiated into human hepatocytes without fusion, *Blood* 106 (2) (2005) 756–763.
- [4] C. Toma, M.F. Pittenger, K.S. Cahill, B.J. Byrne, P.D. Kessler, Human mesenchymal stem cells differentiate to a cardiomyocyte phenotype in the adult murine heart, *Circulation* 105 (1) (2002) 93–98.
- [5] M. Dominici, K. Le Blanc, I. Mueller, I. Slaper-Cortenbach, F. Marini, D. Krause, R. Deans, A. Keating, D. Prockop, E. Horwitz, Minimal criteria for defining multipotent mesenchymal stromal cells. The International Society for Cellular Therapy position statement, *Cytotherapy* 8 (4) (2006) 315–317.
- [6] R. Hass, C. Kasper, S. Böhm, R. Jacobs, D. Populations, Sources of human mesenchymal stem cells (msc). A comparison of adult and neonatal tissue-derived msc, *Cell Commun. Signal* 9 (1) (2011) 12.
- [7] D.G. Phinney, Functional heterogeneity of mesenchymal stem cells: implications for cell therapy, *J. Cell. Biochem.* 113 (9) (2012) 2806–2812.
- [8] M. Gazdic, V. Volarevic, N. Arsenijevic, M. Stojkovic, Mesenchymal stem cells: a friend or foe in immune-mediated diseases, *Stem Cell Rev. Rep.* 11 (2) (2015) 280–287.
- [9] R. Abdi, P. Fiorina, C.N. Adra, M. Atkinson, M.H. Sayegh, Immunomodulation by mesenchymal stem cells: a potential therapeutic strategy for type 1 diabetes, *Diabetes* 57 (7) (2008) 1759–1767.
- [10] S. Shi, P. Bartold, M. Miura, B. Seo, P. Robey, S. Gronthos, The efficacy of mesenchymal stem cells to regenerate and repair dental structures, *Orthod. Craniofac. Res.* 8 (3) (2005) 191–199.
- [11] E.A.A. Neel, W. Chrzanowski, V.M. Salih, H.W. Kim, J.C. Knowles, Tissue engineering in dentistry, *J. Dent.* 42 (8) (2014) 915–928.
- [12] H. Egusa, W. Sonoyama, M. Nishimura, I. Atsuta, K. Akiyama, Stem cells in dentistry-part ii: clinical applications, *J. Prosthodont. Res.* 56 (4) (2012) 229–248.
- [13] T. Kukulj, D. Trivanović, I.O. Djordjević, S. Mojsilović, J. Krstić, H. Obradović, S. Janković, J.F. Santibanez, A. Jauković, D. Bugarski, Lipopolysaccharide can modify differentiation and immunomodulatory potential of periodontal ligament stem cells via erk1,2 signaling, *J. Cell. Physiol.* 233 (1) (2018) 447–462.
- [14] M. Miletić, S. Mojsilović, I. Okić-Djordjević, T. Kukulj, A. Jauković, J. Santibanez, G. Jovčić, D. Bugarski, Mesenchymal stem cells isolated from human periodontal ligament, *Arch. Biol. Sci.* 66 (1) (2014) 261–271.
- [15] A. Klimczak, U. Kozłowska, Mesenchymal stromal cells and tissue-specific progenitor cells: their role in tissue homeostasis, *Stem Cells Int.* 2016 (2016) 1–11.
- [16] M. Shimono, T. Ishikawa, H. Ishikawa, H. Matsuzaki, S. Hashimoto, T. Muramatsu, K. Shima, K.I. Matsuzaka, T. Inoue, Regulatory mechanisms of periodontal regeneration, *Microsc. Res. Tech.* 60 (5) (2003) 491–502.
- [17] A. Nanci, D.D. Bosshardt, Structure of periodontal tissues in health and disease, *Periodontol.* 2000 40 (1) (2006) 11–28.
- [18] T. Iwata, M. Yamato, Z. Zhang, S. Mukobata, K. Washio, T. Ando, J. Feijen, T. Okano, I. Ishikawa, Validation of human periodontal ligament-derived cells as a reliable source for cytotherapeutic use, *J. Clin. Periodontol.* 37 (12) (2010) 1088–1099.
- [19] D. Trivanović, A. Jauković, B. Popović, J. Krstić, S. Mojsilović, I. Okić-Djordjević, T. Kukulj, H. Obradović, J.F. Santibanez, D. Bugarski, Mesenchymal stem cells of different origin: comparative evaluation of proliferative capacity, telomere length and pluripotency marker expression, *Life Sci.* 141 (2015) 61–73.
- [20] A. Downes, R. Mouras, A. Elfick, Optical spectroscopy for noninvasive monitoring of stem cell differentiation, *Biomed. Res. Int.* 2010 (2010) 1–10.
- [21] A. Downes, R. Mouras, P. Bagnaninchi, A. Elfick, Raman spectroscopy and cirs microscopy of stem cells and their derivatives, *J. Raman Spectrosc.* 42 (10) (2011) 1864–1870.
- [22] J.W. Chan, D.K. Lieu, Label-free biochemical characterization of stem cells using vibrational spectroscopy, *J. Biophotonics* 2 (11) (2009) 656–668.
- [23] I. Nottingher, I. Bisson, A.E. Bishop, W.L. Randle, J.M. Polak, L.L. Hench, In situ spectral monitoring of mrna translation in embryonic stem cells during differentiation in vitro, *Anal. Chem.* 76 (11) (2004) 3185–3193.
- [24] C. Aksoy, F. Severcan, Role of vibrational spectroscopy in stem cell research, *J. Spectrosc.* 27 (3) (2012) 167–184.
- [25] E. Brauchle, K. Schenke-Layland, Raman spectroscopy in biomedicine-non-invasive in vitro analysis of cells and extracellular matrix components in tissues, *Biotechnol. J.* 8 (3) (2013) 288–297.
- [26] H.G. Schulze, S.O. Konorov, N.J. Caron, J.M. Piret, M.W. Blades, R.F. Turner, Assessing differentiation status of human embryonic stem cells noninvasively using Raman microspectroscopy, *Anal. Chem.* 82 (12) (2010) 5020–5027.
- [27] A. Ghita, F.C. Pascut, V. Sottile, C. Denning, I. Nottingher, Applications of Raman micro-spectroscopy to stem cell technology: label-free molecular discrimination and monitoring cell differentiation, *EPJ Techniques Instrum.* 2 (1) (2015) 1–14.
- [28] H. Bai, P. Chen, H. Fang, L. Lin, G. Tang, G. Mu, W. Gong, Z. Liu, H. Wu, H. Zhao, et al. Detecting viability transitions of umbilical cord mesenchymal stem cells by Raman micro-spectroscopy, *Laser Phys. Lett.* 8 (1) (2011) 78–84.
- [29] H.K. Chiang, F.Y. Peng, S.C. Hung, Y.C. Feng, In situ Raman spectroscopic monitoring of hydroxyapatite as human mesenchymal stem cells differentiate into osteoblasts, *J. Raman Spectrosc.* 40 (5) (2009) 546–549.
- [30] E. Azrad, D. Zahor, R. Vago, Z. Nevo, R. Doron, D. Robinson, L.A. Gheber, S. Rosenwaks, I. Bar, Probing the effect of an extract of elk velvet antler powder on mesenchymal stem cells using Raman microspectroscopy: enhanced differentiation toward osteogenic fate, *J. Raman Spectrosc.* 37 (4) (2006) 480–486.
- [31] C. Krafft, J. Popp, The many facets of Raman spectroscopy for biomedical analysis, *Anal. Bioanal. Chem.* 407 (3) (2015) 699–717.
- [32] B.S. Kim, C.C.I. Lee, J.E. Christensen, T.R. Huser, J.W. Chan, A.F. Tarantal, Growth, differentiation, and biochemical signatures of rhesus monkey mesenchymal stem cells, *Stem Cells Dev.* 17 (1) (2008) 185–198.
- [33] L. Harkness, S.M. Novikov, J. Beermann, S.I. Bozhevolnyi, M. Kassem, Identification of abnormal stem cells using Raman spectroscopy, *Stem Cells Dev.* 21 (12) (2012) 2152–2159.
- [34] A. Rygula, K. Majzner, K.M. Marzec, A. Kaczor, M. Pilarczyk, M. Baranska, Raman spectroscopy of proteins: a review, *J. Raman Spectrosc.* 44 (8) (2013) 1061–1076.
- [35] K. Czamara, K. Majzner, M. Pacia, K. Kochan, A. Kaczor, M. Baranska, Raman spectroscopy of lipids: a review, *J. Raman Spectrosc.* 46 (1) (2015) 4–20.
- [36] K. Maquelin, C. Kirschner, L.-P. Choo-Smith, N. van den Braak, H. Endtz, D. Naumann, G. Puppels, Identification of medically relevant microorganisms by vibrational spectroscopy, *J. Microbiol. Methods* 51 (3) (2002) 255–271.
- [37] G. Clemens, J.R. Hands, K.M. Dorling, M.J. Baker, Vibrational spectroscopic methods for cytology and cellular research, *Analyst* 139 (18) (2014) 4411–4444.
- [38] Q. Matthews, A. Jirasek, J. Lum, X. Duan, A.G. Brolo, Variability in Raman spectra of single human tumor cells cultured in vitro: correlation with cell cycle and culture confluency, *Appl. Spectrosc.* 64 (8) (2010) 871–887.
- [39] Z. Movasaghi, S. Rehman, I.U. Rehman, Raman spectroscopy of biological tissues, *Appl. Spectrosc. Rev.* 42 (5) (2007) 493–541.
- [40] T. Ichimura, K.F. Liang-da Chiu, S. Kawata, T.M. Watanabe, T. Yanagida, H. Fujita, Visualizing cell state transition using Raman spectroscopy, *PLoS one* 9 (1) (2014) 1–8.
- [41] E. Brauchle, S. Noor, E. Holtorf, C. Garbe, K. Schenke-Layland, C. Busch, Raman spectroscopy as an analytical tool for melanoma research, *Clin. Exp. Dermatol.* 39 (5) (2014) 636–645.
- [42] M. Pudlas, E. Brauchle, T.J. Klein, D.W. Huttmacher, K. Schenke-Layland, Non-invasive identification of proteoglycans and chondrocyte differentiation state by Raman microspectroscopy, *J. Biophotonics* 6 (2) (2013) 205–211.
- [43] G.S. Mandair, M.D. Morris, Contributions of Raman spectroscopy to the understanding of bone strength, *BoneKey Reports* 4 (620) (2015) 1–8.
- [44] J. Kobilak, A. Dinnyes, A. Memic, A. Khademhosseini, A. Mobasher, Mesenchymal stem cells: identification, phenotypic characterization, biological properties and potential for regenerative medicine through biomaterial micro-engineering of their niche, *Methods* 99 (2016) 62–68.



Република Србија
Универзитет у Београду
Технолошко-металуршки факултет
Д.Бр.2013/4001
Датум: 12.04.2019. године

На основу члана 29. Закона о општем управном поступку („Сл. гласник РС”, бр.18/2016) и службене евиденције издаје се

УВЕРЕЊЕ

Лазаревић (Јован) Јасмина, бр. индекса 2013/4001, рођена 05.10.1985. године, Београд, Београд-Савски Венац, Република Србија, уписана школске 2018/2019. године, у статусу: самофинансирајући; тип студија: Докторске академске студије; студијски програм: Биохемијско инжењерство и биотехнологија.

Према Статуту факултета студије трају (број година): три године.

Рок за завршетак студија: у троструком трајању студија.

Ово се уверење може употребити за регулисање војне обавезе, издавање визе, права на дечији додатак, породичне пензије, инвалидског додатка, добијања здравствене књижице, легитимације за повлашћену возњу и стипендије.



Овлашћено лице факултета



Република Србија
Универзитет у Београду
Технолошко-металуршки факултет
Д.Бр.2013/4001
Датум: 12.04.2019. године

На основу члана 29. Закона о општем управном поступку („Сл. гласник РС”, бр.18/2016) и службене евиденције издаје се

УВЕРЕЊЕ

Лазаревић (Јован) Јасмина, бр. индекса 2013/4001, рођена 05.10.1985. године, Београд, Београд-Савски Венац, Република Србија, уписана школске 2018/2019. године, у статусу: самофинансирајући; тип студија: Докторске академске студије; студијски програм: Биохемијско инжењерство и биотехнологија.

Према Статуту факултета студије трају (број година): три године.

Рок за завршетак студија: у троструком трајању студија.

Ово се уверење може употребити за регулисање војне обавезе, издавање визе, права на дечији додатак, породичне пензије, инвалидског додатка, добијања здравствене књижице, легитимације за повлашћену возњу и стипендије.



Овлашћено лице факултета

РЕПУБЛИКА СРБИЈА



УНИВЕРЗИТЕТ У БЕОГРАДУ
ФАРМАЦЕУТСКИ ФАКУЛТЕТ

ДИПЛОМА
О СТЕЧЕНОМ ВИСОКОМ ОБРАЗОВАЊУ

Јасмина Јован Цвејић

Рођена 05.10.1985. године у Београду, Савски венац, Република Србија,
уписана 2004/05. школске године, а дана 29.04.2011. године
завршила је основне студије на Фармацеутском факултету,
смер за фармацеуте, са просечном оценом 8,26 (осам и 26/100)
у току студија и одбранила дипломски рад са оценом 10 (десет).

На основу тога издаје јој се ова диплома о стеченом
високом образовању и стручном називу

Дипломирани фармацеут

Редни број из евиденције о издатим дипломама 4934

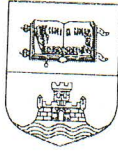
У Београду 29.04.2011. године

Декан

Проф. др Нада Ковачевић

Ректор

Проф. др Бранко Ковачевић



УНИВЕРЗИТЕТ У БЕОГРАДУ

Студентски трг 1, 11000 Београд, Република Србија
Тел.: 011 3207400; Факс: 011 2638912; E-mail: officebu@rect.bg.ac.rs

ВЕЋЕ НАУЧНИХ ОБЛАСТИ
ТЕХНИЧКИХ НАУКА

Београд, 25.3.2019. године
02 број: 61206-1329/2-19
ЛД

На основу члана 48. став 5. тачка 3. Статута Универзитета у Београду ("Гласник Универзитета у Београду", број 201/18) и чл. 14. – 21. Правилника о већима научних области на Универзитету у Београду ("Гласник Универзитета у Београду", број 134/07, 150/09, 158/10, 164/11, 165/11, 180/14, 195/16 и 197/17), а на захтев Технолошко-металуршког факултета, број: 35/82 од 14.3.2019. године, Веће научних области техничких наука, на седници одржаној 25.3.2019. године, донело је

ОДЛУКУ

ДАЈЕ СЕ САГЛАСНОСТ на предлог теме докторске дисертације Јасмине Лазаревић, под називом: „Раманова спектроскопија фармаколошки активних супстанци и биокатализатора“.

ПРЕДСЕДНИК ВЕЋА

Проф. др Јован Филиповић

Доставити:

- Факултету,
- Архиви Универзитета.

Бр. 20/29

08. 06. 2015 год.
БЕОГРАД

Na osnovu člana 38 Statuta Tehnološko-metalurškog fakulteta, na osnovu Odluke Nastavno-naučnog veća sa sednice od 04. juna 2015. godine, a u skladu sa čl. 82 Zakona o naučno-istraživačkoj delatnosti, donosi se

РЕШЕЊЕ

JASMINA LAZAREVIĆ, diplomirani farmaceut, stekla je uslov za izbor u zvanje **ISTRAŽIVAČ SARADNIK**.

Образложење

Na osnovu Odluke br. 35/249 Nastavno-naučnog veća sa sednice od 04. juna 2015. godine skladu sa čl. 73 i 82 Zakona o naučno-istraživačkoj delatnosti, doneto je rešenje kao u dispozitivu.

Protiv ovog rešenja može se uložiti prigovor Nastavno-naučnom veću fakulteta u roku od 15 dana prijema rešenja.

Dostaviti:

Imenovanoj 2x
Kadrovskoj službi 2x
Arhivi



Prof. dr Đorđe Janačković



Република Србија
Универзитет у Београду
Технолошко-металуршки факултет

2018
21.02.2017

На основу чл. 94. Закона о високом образовању, чл. 65. Статута Технолошко-металуршког факултета, а на лични захтев студента, доноси се

РЕШЕЊЕ

Усваја се захтев који је упутио, **Јасмина Лазаревић**, студент ДАС, број индекса 2013/4001, и одобрава мировање права и обавеза у школској 2016/2017. години, на основу приложених докумената.

Декан

Проф. др Ђорђе Јанаћковић